FUNGAL INFECTION

Rewilding of laboratory mice enhances granulopoiesis and immunity through intestinal fungal colonization

Ying-Han Chen[1]†, Frank Yeung[1]†, Keenan A. Lacey[2], Kimberly Zaldana[1], Jian-Da Lin[3], Gavyn Chern Wei Bee[2], Caroline McCauley[2], Ramya S. Barre[4], Shen-Huan Liang[5], Christina B. Hansen[4], Alexander E. Downie[4], Kyle Tio[1], Jeffrey N. Weiser[2,6], Victor J. Torres[2,6], Richard J. Bennett[5], P'ng Loke[7]*, Andrea L. Graham[4]*, Ken Cadwell[8,9,10]*

The paucity of blood granulocyte populations such as neutrophils in laboratory mice is a notable difference between this model organism and humans, but the cause of this species-specific difference is unclear. We previously demonstrated that laboratory mice released into a seminatural environment, referred to as rewilding, display an increase in blood granulocytes that is associated with expansion of fungi in the gut microbiota. Here, we find that tonic signals from fungal colonization induce sustained granulopoiesis through a mechanism distinct from emergency granulopoiesis, leading to a prolonged expansion of circulating neutrophils that promotes immunity. Fungal colonization after either rewilding or oral inoculation of laboratory mice with *Candida albicans* induced persistent expansion of myeloid progenitors in the bone marrow. This increase in granulopoiesis conferred greater long-term protection from bloodstream infection by gram-positive bacteria than by the trained immune response evoked by transient exposure to the fungal cell wall component β-glucan. Consequently, introducing fungi into laboratory mice may restore aspects of leukocyte development and provide a better model for humans and free-living mammals that are constantly exposed to environmental fungi.

INTRODUCTION

Laboratory mice are extensively used for studying how the microbiota contributes to the differentiation and function of the immune system (*1*–*5*). However, laboratory mice kept in ultrahygienic specific pathogen–free (SPF) facilities lack the microbial exposure that humans and free-living mammals experience in a more complex environment. The artificial laboratory condition may give rise to differences between mice and humans in terms of proportions of leukocyte subsets, immune response to microbial challenges, and pathogenesis outcomes (*6*–*8*). Consistent with a role for microbes in this discrepancy, laboratory mice display a more mature immune system resembling that of an adult human after serial infection by pathogens or cohousing with "dirty" mice harboring pathogens (*9*–*12*). In addition to lack of exposure to disease-causing pathogens, an artificial microbiota composition may also contribute to the lack of concordance between observations made in laboratory mice and humans. Mice reconstituted with microbiota from wild mice through fecal microbiome transplantation (FMT) or vertical transmission better recreate the unresponsiveness to immunotherapies that failed in clinical trials and display an altered course of influenza infection and colorectal tumorigenesis in these respective disease settings (*13*, *14*).

The gut microbiota consists of multiple kingdoms of diverse unicellular organisms and, when the term is applied to agents transmitted through cohousing and FMTs, can include viruses and multicellular parasites with immunogenic properties. Thus, the respective contribution of symbiotic bacteria versus other microbial agents in the wild microbiota to immune development requires clarification. Another barrier toward investigating the natural microbiota is that wild mice harbor both environmental microbes and transmissible agents that straddle the line between commensal and pathogen. To address these issues, we recently established a mesocosm system termed "rewilding" in which laboratory mice experience a seminatural environment through release into an outdoor enclosure facility (*15*). A key feature of this outdoor enclosure facility is that the fencing system prevents contact with wild rodents that potentially harbor pathogens while allowing the mice to freely explore and encounter the natural plant and insect fauna. Hence, rewilded laboratory mice are exposed to environmental microbes but remain seronegative for pathogens excluded from SPF facilities (*16*). We previously demonstrated that rewilded mice display hallmarks of increased immune activation compared with matched control laboratory mice, which included a notable expansion of granulocytes, a group of myeloid lineage white blood cells that include first responders such as neutrophils (*16*, *17*). The gut microbiota of rewilded mice displayed >100-fold increases in fungal burden compared with laboratory mice, and transferring fungi

[1]Kimmel Center for Biology and Medicine at the Skirball Institute, New York University Grossman School of Medicine, New York, NY 10016, USA. [2]Department of Microbiology, New York University Grossman School of Medicine, New York, NY 10016, USA. [3]Department of Biochemical Science and Technology, College of Life Science, National Taiwan University, Taipei City, Taiwan. [4]Department of Ecology and Evolutionary Biology, Princeton University, Princeton, NJ 08544, USA. [5]Department of Molecular Microbiology and Immunology, Brown University, Providence, RI 02912, USA. [6]Antimicrobial-Resistant Pathogens Program, New York University Grossman School of Medicine, New York, NY 10016, USA. [7]Laboratory of Parasitic Diseases, National Institute of Allergy and Infectious Diseases, National Institutes of Health, Bethesda, MD 20892, USA. [8]Division of Gastroenterology and Hepatology, Department of Medicine, University of Pennsylvania Perelman School of Medicine, Philadelphia, PA 19104, USA. [9]Department of Systems Pharmacology and Translational Therapeutics, University of Pennsylvania Perelman School of Medicine, Philadelphia, PA 19104, USA. [10]Department of Pathology and Laboratory Medicine, University of Pennsylvania Perelman School of Medicine, Philadelphia, PA 19104, USA.
*Corresponding author. Email: ken.cadwell@pennmedicine.upenn.edu (K.C.); png.loke@nih.gov (P.L.); algraham@princeton.edu (A.L.G.)
†These authors contributed equally to this work.

isolated from feces of rewilded mice into laboratory mice reproduced the increase in peripheral granulocytes. We were able to mimic this effect by colonizing the intestines of laboratory mice with *Candida albicans*, a model fungus that is commonly detected in the human gut.

C. albicans, a gut commensal and opportunistic pathogen, colonizes most individuals since childhood (*18*–*20*). The transition from yeast to hyphal cell morphology has been shown to regulate the balance between commensalism and invasive infection in the gastrointestinal tract (*21*–*27*). Commensal *C. albicans* can stimulate the differentiation of $CD4^+$ T helper 17 (T_H17) cells to improve immunity, fortify the intestinal barrier, and regulate social behavior (*28*–*33*). In addition to this adaptive immune response mediated by lymphocytes during gut colonization, bloodstream *C. albicans* infection can prime an innate immune memory response mediated by the myeloid compartment termed trained immunity. To meet the high demand for phagocytes to contain invasive pathogens, progenitors in the bone marrow (BM) rapidly ramp up the differentiation of myeloid cells through the process of emergency granulopoiesis, which returns to baseline levels after resolution of the infection (*34*–*36*). However, a number of studies showed that the response to *C. albicans* or fungal products has long-term consequences due to the reprogramming of the myeloid compartment, resulting in an enhanced response to reinfection (*35*, *37*–*42*). In this setting, β-glucan, a universal-fungal cell wall component, activates dectin-1 and the signaling adaptor caspase recruitment domain-containing protein 9 (CARD9) to alter chromatin accessibility in trained monocytes and macrophages, which enhances production of inflammatory cytokines (*41*, *43*, *44*). Although T_H17 differentiation after local activation of $CX3CR1^+$ mononuclear phagocytes during intestinal colonization by *C. albicans* is also dependent on dectin-1 (*45*), it is unclear whether blood granulocyte expansion in rewilded mice involves this pathway. Similarly, the qualitative differences between mobilization of granulocytes after gut colonization versus transient bloodstream exposure to fungi require a better understanding.

Here, we found that *C. albicans* inoculation and fungal colonization after rewilding of laboratory mice increased the number and frequency of multipotent progenitors (MPPs) and the myeloid-biased MPP3 subset in the BM. Optimal expansion of MPP3s required interleukin-6 (IL-6) but were unexpectedly independent of dectin-1 and T_H17 pathways. This enhanced granulopoiesis led to an increase in circulating $CD62L^{hi}CXCR4^{lo}$ neutrophils in *C. albicans*–colonized laboratory mice and rewilded mice, as well as increases in eosinophils exclusively in rewilded mice. A yeast-locked *C. albicans* mutant was unable to induce MPP3s in the BM and neutrophils in the blood, which was attributed to the lack of production of the hypha-associated factor candidalysin. In contrast to transient β-glucan–induced granulopoiesis, fungal colonization sustained the increased granulopoiesis, which was reflected by persistently high levels of peripheral neutrophils. Consequently, *C. albicans*–colonized mice displayed prolonged protection against *Staphylococcus aureus* bloodstream infection and yielded greater immunity at later time points when compared side by side to the previously described β-glucan–induced trained immunity model. Together, these findings implicate intestinal fungi in continuously remodeling myeloid cell development in the BM and suggest that environmental fungi may, in part, correct the differences between laboratory mice and humans.

RESULTS

Intestinal *C. albicans* colonization enhances granulopoiesis in the BM

We previously found that inoculating germ-free mice or antibiotics-treated laboratory mice with *C. albicans* (SC5314) mimics the increase in blood granulocytes observed in rewilded mice that are exposed to fungi, such as *Aspergillus* spp., in a more natural environment. *C. albicans* is a genetically tractable model fungus with isogenic mutants available for study, and its use allowed us to compare our findings with the literature on fungal colonization of the gut. Therefore, we used rewilding and *C. albicans* colonization models interchangeably in this study to cross-validate key observations regarding the mechanism of granulocyte expansion. Although we previously established that the increase in blood granulocytes in the antibiotics pretreatment model of *C. albicans* colonization was due to an increase in neutrophils ($CD11b^+Ly6G^+$), we did not examine additional cell surface markers that inform neutrophil biology. Surface levels of the chemokine receptors CXCR4 and cell adhesion molecule CD62L increase and decrease, respectively, as neutrophils age (*46*, *47*). We found that the ratio of the newly released population ($CD62L^{hi}CXCR4^{lo}$) of neutrophils to the aged population ($CD62L^{lo}CXCR4^{hi}$) of neutrophils substantially increased in antibiotics-treated *C. albicans*–colonized mice compared with noncolonized control mice, suggesting that fungal colonization increases the number of fresh neutrophils in the blood (Fig. 1A and fig. S1A). These results raise the possibility that *C. albicans* enhances the production of neutrophils.

Hematopoietic stem cells (HSCs) are defined as the $Lin^-Sca\text{-}1^+c\text{-}Kit^+$ (LSK) fraction of the BM that give rise to nonself-renewing MPPs. MPPs, composed of three subsets, give rise to leukocyte populations. MPP2 and MPP3 are myeloid-biased MPP subsets that develop toward erythrocyte/megakaryocyte and monocyte/granulocyte lineages, respectively, whereas MPP4 commits to lymphoid lineage development (*48*, *49*). To examine whether the expansion of peripheral neutrophils is attributed to the response of the myeloid progenitor pool, we used flow cytometry to analyze the BM in germ-free mice and antibiotics-treated mice colonized by *C. albicans*. Compared with mock-treated controls, germ-free mice 21 days after oral gavage with *C. albicans* displayed increases in the total cellularity of the femoral BM and the number of MPPs ($CD48^+CD150^-LSK$) but not HSCs (Fig. 1, B to D, and fig. S1B). In addition, the number of myeloid-biased MPP3 subset ($Flt3^-CD150^-CD48^+LSK$) that gives rise to neutrophils was greatly increased (Fig. 1, E and F). Although absolute number of lymphocyte precursor MPP4s ($Flt3^-CD150^-CD48^+LSK$) increased, the ratio of MPP4 to MPP3 was reduced (Fig. 1G), indicating a skewing toward granulocyte differentiation. *C. albicans*–colonized antibiotic-treated mice also displayed a comparable increase in total MPPs and the MPP3 subset but not MPP4 (fig. S1, C and D), demonstrating that fungal colonization favors myeloid-lineage commitment in both the germ-free and antibiotics pretreatment models. Treatment of *C. albicans* mono-associated mice with the antifungal drug fluconazole decreased fungal burden and reduced neutrophils in the blood along with the frequency of myeloid progenitor pools (Fig. 1, H to J, and fig. S1E). These results suggest that persistent colonization with fungi is essential to maintain the elevated granulopoiesis.

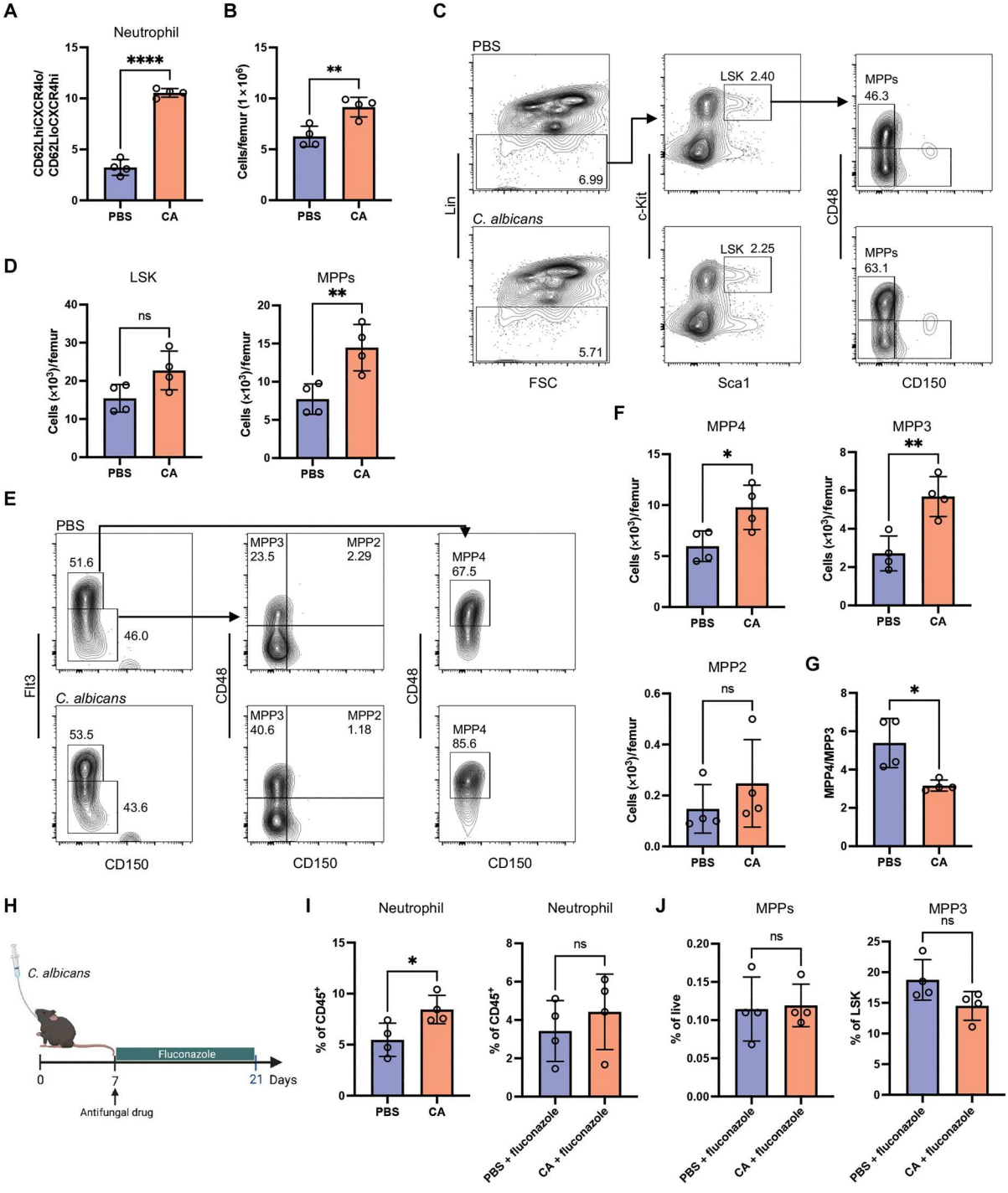

Fig. 1. Inoculation of laboratory mice with *C. albicans* drives expansion of myeloid progenitors. (**A**) Ratio of newly released ($CD62L^{hi}CXCR4^{lo}$) population to aged ($CD62L^{lo}CXCR4^{hi}$) population of $Ly6G^{+}$ peripheral neutrophils from antibiotic-treated mice 21 days after inoculation with PBS or *C. albicans*. $n = 4$ mice per group. (**B**) The cellularity of total BM cells from germ-free mice 21 days after inoculation with PBS or *C. albicans*. $n = 4$ mice per group. (**C**) Representative flow cytometry plots depicting gating strategy for HSCs and progenitors in BM from germ-free mice inoculated with PBS or *C. albicans*. LSK cells were gated from Lin^{-} cells and characterized as $Sca1^{+}$c-Kit^{+} cells. A subpopulation of LSK was further characterized as MPP ($CD48^{+}CD150^{-}$LSK). (**D**) Quantification of number of LSK and MPPs from (C). $n = 4$ mice per group. (**E**) Representative flow cytometry plots depicting gating strategy used to identify MPP subsets in BM from germ-free mice inoculated with PBS or *C. albicans*. MPP4 cells were gated on $Flt3^{+}$LSK and identified by CD48 and CD150. MPP3 and MPP2 cells were gated on $Flt3^{-}$LSK and identified by CD48 and CD150. (**F**) Quantification of the number of MPP subsets from (E). (**G**) Ratio of MPP4 to MPP3. (**H**) Germ-free mice were administrated fluconazole in the drinking water continuously starting from day 7 after inoculation with PBS or *C. albicans*. Blood and BM analysis were performed day 21 after inoculation. $n = 4$ mice per group. (**I**) Frequency of neutrophils in the peripheral blood of germ-free mice treated as in (H). (**J**) Frequency of MPPs and MPP3 in the BM of germ-free mice treated as in (H). Dots in bar graphs correspond to individual mice. Mean and SD are shown. $^{*}P < 0.05$, $^{**}P < 0.01$, and $^{****}P < 0.0001$ by two-tailed Student's *t* test between groups. ns, not significant.

Rewilding increases granulopoiesis

To determine whether granulopoiesis is enhanced after exposure to the natural environment, we performed an independent rewilding experiment in which 6- to 8-week-old SPF laboratory mice were released into the enclosure and captured 6 weeks later, at which point their immune profile was compared with littermate controls kept in the conventional animal facility. Given that the previous rewilding experiment was performed in 2017, we first confirmed that granulocyte expansion was reproducible and not subject to year-to-year variation in the local environment of the outdoor facility (e.g., vegetation, weather, etc.). Despite the 2-year interval between experiments, rewilded mice displayed a similar expansion of granulocytes (SSC^{hi}) in the periphery as before (Fig. 2A). Our previous rewilding experiment did not include flow cytometry markers for distinguishing granulocyte subsets. Although the increase in blood neutrophils was not statistically significant, a positive correlation between the abundance of circulating neutrophils and fungal burden was still observed in rewilded mice (fig. S2A). In addition, neutrophils from rewilded mice displayed a dramatically altered cell surface staining for CD62L and CXCR4 compared with laboratory controls indicative of an increase in newly generated ($CD62L^{hi}$ $CXCR4^{lo}$) cells (Fig. 2, B and C), similar to *C. albicans*–colonized laboratory mice. Rewilded mice displayed a substantial increase in eosinophils that was not observed in *C. albicans*–colonized laboratory mice (Fig. 2A and fig. S2B). This difference could be explained by the presence of other fungal taxa in the outdoor enclosure. To test this possibility, we gavaged laboratory mice every other day repeatedly for 2 weeks with a consortium of "wild" fungi that we previously isolated from rewilded mice (*16*) and found that this treatment induced an increase in peripheral eosinophils (fig. S2C). Thus, we believe that *C. albicans* is useful for mechanistic probing how fungi induce neutrophil expansion, whereas wild fungi might better recapitulate the full effect of rewilding. Consistent with our previous finding that rewilded mice harbored a significant increase in stool fungal burden, we readily observed the presence of fungi associated with the mucus layer in the small intestine of rewilded mice. In contrast, fungi were nearly undetectable in laboratory mice (Fig. 2D). These results highlight the reproducibility of granulocyte expansion and fungal colonization in our rewilding system, and also identify eosinophils as a uniquely expanded population in mice captured from outdoors.

Like *C. albicans*–colonized mice, rewilded mice showed a significantly increased BM cellularity and the number and frequency of MPPs. In addition, rewilded mice displayed a higher absolute number but not proportion of HSCs than laboratory mice (Fig. 2, E to G, and fig. S2D). Rewilding also led to an increase in the number and frequency of myeloid-biased MPP3s and not lymphoid-biased MPP4s (Fig. 2, H and I, and fig. S2E). In contrast to the periphery where the neutrophils are mature ($Ly6G^{+}$), neutrophils in the BM can be segregated into mature $Ly6G^{+}CXCR2^{+}$ and immature $Ly6G^{lo/+}CXCR2^{-}$ populations (*50*). Using these markers, we found the frequency of immature neutrophils increased and mature neutrophils decreased in the BM of rewilded mice compared with laboratory mice (fig. S2F). In human BM, the majority of neutrophils are immature. Therefore, we believe that fungal colonization brings the steady state of neutrophil development in laboratory mice to more closely resemble human BM development. Overall, these results demonstrate that rewilding leads to enhanced granulopoiesis giving rise to younger neutrophils in the periphery, similar to inoculation of laboratory mice with *C. albicans*.

Fungal colonization of the gut induces sustained changes to the host immune system

To determine whether the time course of granulopoiesis differs between invasive infection and gut colonization, we attempted to compare the immune response between oral and intravenous inoculation with *C. albicans*. Because the gut colonization model involves antibiotic pretreatment, mice received the same antibiotics regimen prior to intravenous injection with a nonlethal dose of *C. albicans*. Unexpectedly, intravenous injection led to similar levels of *C. albicans* gut colonization as the oral route of inoculation (Fig. 3A). Thus, we concluded that the intravenous *C. albicans* injection model is inappropriate for investigating transient exposure to fungi and turned to a simpler established model of acute antifungal responses.

β-Glucan is an abundant fungal cell wall polysaccharide that elicits host responses through activating innate immune receptors such as dectin-1 (*51*, *52*). Therefore, we performed a time course analysis comparing the effect of intraperitoneal injection with β-glucan and oral gavage with *C. albicans* in antibiotics-treated mice. Intraperitoneal injection of β-glucan led to expansion of SSC^{hi} granulocytes and neutrophils in the blood as early as 24 hours after treatment compared with control mice, which returned to baseline levels by day 3 (Fig. 3, B to D). In contrast, the frequency of peripheral granulocytes and neutrophils reached a plateau at day 3 in mice orally inoculated with *C. albicans* and remained high throughout the course of the experiment, matching the stable levels of colonization observed in the stool (Fig. 3, C to E). The number of blood eosinophils and monocytes were largely unaffected by β-glucan injection and *C. albicans* gut colonization (fig. S3, A and B). MPPs and MPP3s in the BM were increased and remained high in mice orally inoculated with *C. albicans*. However, different from the time course of neutrophil expansion in the blood, the increase in these progenitor populations after β-glucan injection led to a gradual decline rather than a steep drop at day 3 (Fig. 3, F and G). These findings indicate that fungal colonization of the gut leads to sustained granulopoiesis and stable expansion of neutrophils, whereas a single intraperitoneal injection of β-glucan induces transient changes.

Fungal colonization enhances granulopoiesis independently of dectin-1 and T_H17 pathways but in a manner dependent on IL-6R signaling

Antigen-presenting cells activated by dectin-1 and other pattern recognition receptors that signal through CARD9 can induce the differentiation of T_H17 cells that mediate neutrophil mobilization through IL-17A (*53*, *54*). Therefore, it is possible that *C. albicans* colonization induces sustained dectin-1 signaling. However, daily intraperitoneal injection of β-glucans for 7 days did not induce a significant increase in peripheral neutrophils and eosinophils (fig. S4A). Although repetitive β-glucan injection induced a slight increase in MPP3s, in contrast to *C. albicans*–colonized mice, MPP2s were also increased and the ratio of MPP4 to MPP3 was comparable to the mock-treated mice (fig. S4. B and C). These results raise the possibility that the effects of intestinal fungal colonization are dectin-1 and CARD9 independent. *C. albicans* colonization still induced increases in MPP3s in the BM and peripheral

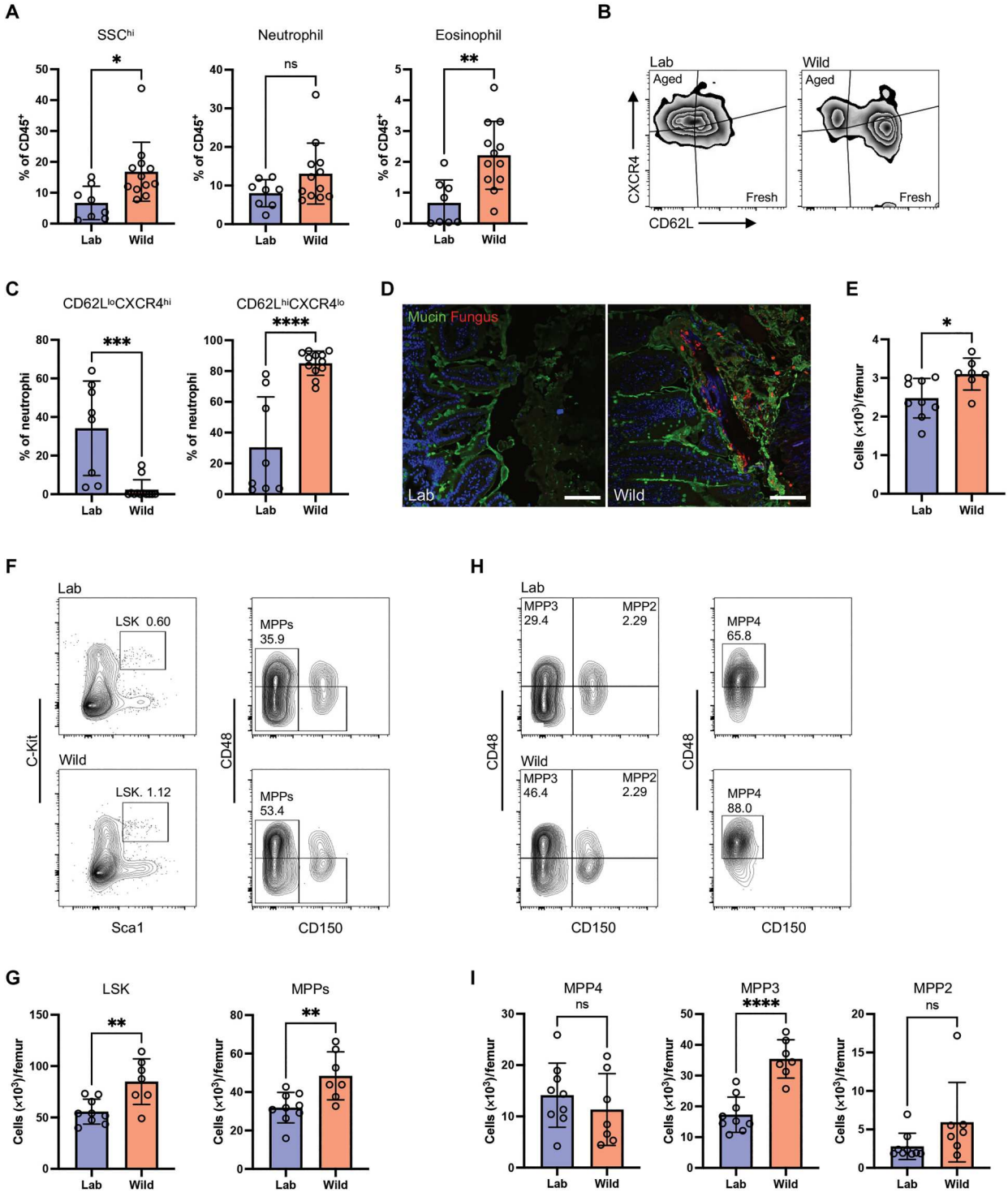

Fig. 2. Rewilding increases granulopoiesis. (**A**) Frequency of granulocytes (SSChi), neutrophils (Ly6G$^+$), and eosinophils (Siglec-F$^+$) in the peripheral blood of rewilded mice (wild) and control mice maintained in the laboratory condition (lab). Neutrophils and eosinophils were gated on Live$^+$CD45$^+$CD11b$^+$. $n = 8$ lab and 12 rewilded mice. (**B**) Representative flow cytometry plots of newly released (CD62L^{hi}CXCR4^{lo}) and aged (CD62L^{lo}CXCR4^{hi}) neutrophils. (**C**) Quantification of proportion of fresh and aged neutrophils. $n = 8$ lab and 12 rewilded mice. (**D**) Confocal images of ileum sections immunostained with anti-candida antibody (nonspecifically labels fungi) and counterstained with FITC-lectins mixture, which binds to oligosaccharide structures of mucins. Scale bars, 100 μm. (**E**) The cellularity of total BM cells from lab and rewilded mice. $n = 9$ lab and 7 rewilded mice (E, G, and I). (**F**) Representative flow cytometry plots of LSK (Lin$^-$cKit$^+$Sca1$^+$) and MPPs (CD48$^+$CD150$^-$LSK). (**G**) Cell number of LSK and MPPs in the BM of lab and rewilded mice. (**H**) Representative flow cytometry plots of MPP4, MPP3, and MPP2. (**I**) Cell number of MPP subsets in the BM of lab and rewilded mice. Dots in bar graphs correspond to individual mice. Mean and SD are shown. *$P < 0.05$, **$P < 0.01$, ***$P < 0.001$, and ****$P < 0.0001$ by two-tailed Student's t test between groups.

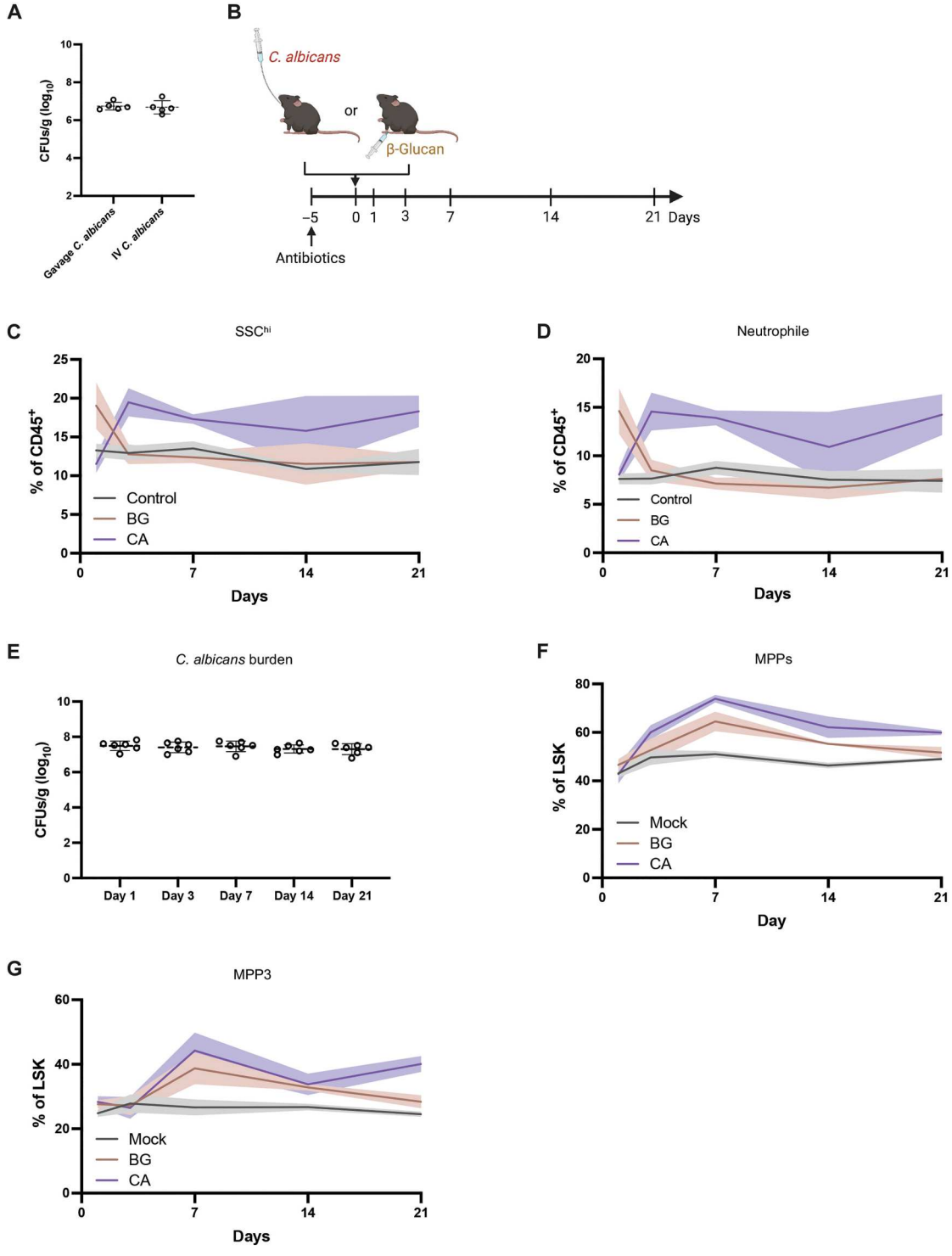

Fig. 3. Intestinal *C. albicans* colonization leads to sustained granulopoiesis. (**A**) CFUs of *C. albicans* in feces from antibiotic-treated mice 21 days after oral inoculation with *C. albicans* or intravenous injection with a nonlethal dose (1×10^4 CFUs). $n = 5$ mice per group. (**B**) Experimental model of *C. albicans* colonization and β-glucan injection in antibiotic-treated mice. Blood and BM were collected on days 1, 3, 14, and 21 of inoculation for flow cytometry analysis. $n = 6$ mice per group. (**C** and **D**) Frequency of granulocytes (SSC^{hi}) and neutrophils in the peripheral blood from mock, *C. albicans*–colonized and β-glucan–injected mice. (**E**) *C. albicans* CFUs in feces collected from antibiotic-treated mice inoculated with *C. albicans* on indicated days. (**F** and **G**) Frequency of MPPs and MPP3 in the BM from mock, *C. albicans*–colonized and β-glucan–injected mice.

neutrophils in mice lacking dectin-1 (*Clec7a*) or CARD9 (Fig. 4A and fig. S4D). Dectin-1− and CARD9-deficient mice displayed similar amounts of *C. albicans* in the stool as their wild-type littermates (Fig. 4B). Also, rewilded dectin-1− and CARD9-deficient mice exhibited enhanced granulopoiesis, including an increased number in MPPs and MPP3, upon being released into the outdoor enclosure (Fig. 4C and fig. S4E). In addition to dectin-1, we also examined the role of Toll-like receptor 2 (TLR2), which recognizes phospho-lipomannans and chitin from the fungal cell wall (*55*, *56*). We found that *C. albicans* colonization induced increases

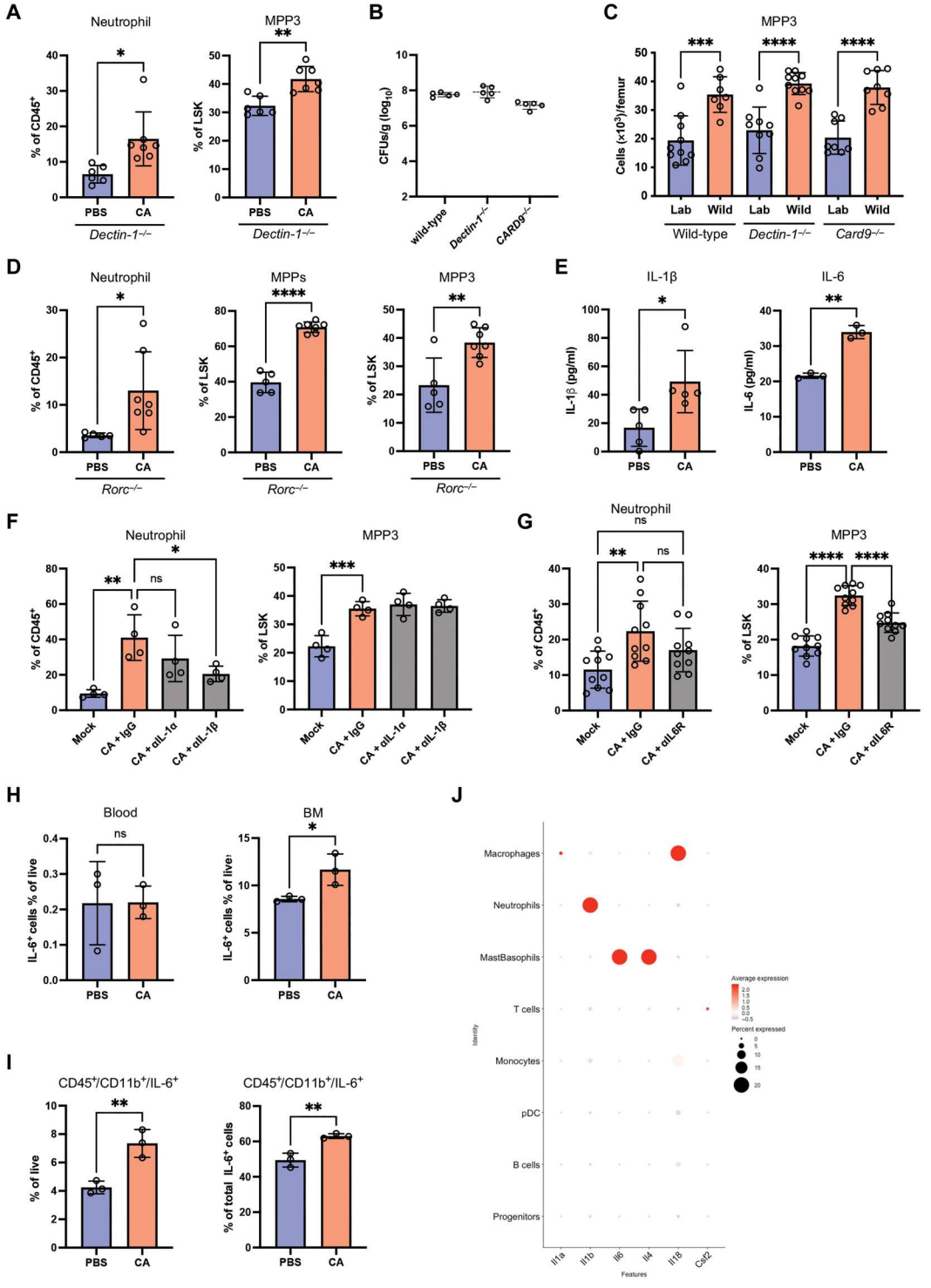

Fig. 4. Fungal colonization enhances granulopoiesis in a manner dependent on IL-6R signaling. (**A**) Frequency of neutrophils in the peripheral blood and MPP3 in the BM from antibiotic-treated *Dectin-1*$^{-/-}$ mice 21 days after inoculation with *C. albicans*. $n = 6$ PBS control and $n = 7$ *C. albicans*–colonized mice. (**B**) Fungal CFUs in feces from *C. albicans*–colonized wild-type, *Dectin-1*$^{-/-}$, and *Card9*$^{-/-}$ mice on day 21. $n = 5$ mice per group. (**C**) Quantification of number of MPP3 in the BM of laboratory and rewilded wild-type ($n = 9$ lab and 7 rewilded mice), *Dectin-1*$^{-/-}$ ($n = 8$ lab and 10 rewilded mice), and *Card9*$^{-/-}$ ($n = 8$ lab and 8 rewilded mice) mice. (**D**) Frequency of neutrophils in the peripheral blood and MPPs and MPP3 in the BM from antibiotic-treated *Rorc*$^{-/-}$ mice 21 days after inoculation with *C. albicans*. $n = 5$ PBS control and $n = 7$ *C. albicans*–colonized mice. (**E**) Quantification of IL-1β ($n = 5$) and IL-6 ($n = 3$) in the BM extracellular fluid from antibiotic-treated mice 21 days after inoculation with PBS or *C. albicans*. (**F**) Frequency of neutrophils in the peripheral blood and MPP3 in the BM on day 7 from mice treated with anti–IL-1α, anti–IL-1β, or IgG isotype control antibodies on days −1, 1, 3, and 5 days after inoculation with *C. albicans*. $n = 4$ mice per group. (**G**) Frequency of neutrophils in the peripheral blood and MPP3 in the BM from mice treated with anti–IL-6R or IgG isotype control antibodies on days −1, 1, 3, and 5 days after inoculation with *C. albicans*. $n = 10$ mice per group. (**H**) Quantification of IL-6$^+$ cells gated on live cells in the peripheral blood and BM from antibiotic-treated mice 21 days after inoculation with PBS or *C. albicans* by flow cytometry. (**I**) Proportion of live IL-6$^+$ cells that are CD45$^+$CD11b$^+$ (left) and quantification of live cells that are IL-6$^+$ myeloid cells (CD45$^+$CD11b$^+$) (right) in the BM from antibiotic-treated mice 21 days after inoculation with PBS or *C. albicans*. (**J**) Cytokine gene expression across cell types identified by scRNA-seq analysis. Dots in bar graphs correspond to individual mice. Mean and SD are shown. *$P < 0.05$, **$P < 0.01$, and ****$P < 0.0001$ by two-tailed Student's *t* test between groups (A, D, E, and H) and ordinary one-way ANOVA with Holm-Šidák multiple comparisons test (C, F, and G). Antibiotic-treated groups (A and D to I).

in MPP3 in the BM and peripheral neutrophils in mice lacking TLR2 (fig. S4F). Similarly, in our previous study (*16*), rewilded mice deficient in nucleotide binding oligomerization domain containing 2 (NOD2), another molecule shown to sense fungi (*57*), exhibited a comparable expansion of granulocytes as rewilded wild-type mice.

IL-17A can promote granulopoiesis by inducing increased circulating levels of granulocyte colony-stimulating factor (G-CSF) (*58*, *59*). Therefore, we examined the possibility that the T_H17 response mediates neutrophil expansion during *C. albicans* gut colonization. As demonstrated by others (*33*, *45*), we observed that *C. albicans* colonization increased IL-17 production by CD4 T cells and the proportion of RoRγt$^+$ CD4 T cells in the small intestine and colon (fig. S4, G and H). However, antibiotics-treated *Rorc*$^{-/-}$ mice, which are deficient in IL-17–producing cells, still displayed an in increase in blood neutrophils and expansion of MPPs and MPP3 in the BM upon *C. albicans* colonization (Fig. 4D). We also found that CD4 T cells in general were dispensable by depleting the CD4 T cells in *C. albicans*–colonized wild-type mice (fig. S4I). Together, these results suggest that *C. albicans* colonization modulates neutrophil development independent of canonical fungal sensing receptors such as dectin-1 and antifungal immune pathways.

Other cytokines are known to regulate the expansion of HSCs and differentiation into myeloid progenitors, such as IL-1, IL-6, and granulocyte-macrophage colony-stimulating factor (GM-CSF) (*60*). As expected, we found that IL-1β and IL-6 were significantly increased in the BM of *C. albicans*–colonized mice (Fig. 4E). We injected IL-1α– or IL-1β–specific neutralizing antibodies to assess their contribution. *C. albicans*–colonized mice undergoing IL-1α or IL-1β blockade displayed equivalent MPP3 levels to isotype control–treated mice; yet, peripheral neutrophils were decreased in the anti–IL-1β–injected mice (Fig. 4F). In contrast, blocking the IL-6 receptor (IL-6R) reduced the *C. albicans*–mediated increase in MPP3. The neutrophil levels of anti–IL-6R–treated *C. albicans*–colonized mice and control mice not colonized by *C. albicans* were similar (Fig. 4G). GM-CSF blockade did not reduce either neutrophils or MPP3 in *C. albicans*–colonized mice (fig. S4J). Therefore, fungal colonization in the gut leading to an increase in granulopoiesis was dependent on IL-6R signaling and independent of IL-1 and GM-CSF. However, IL-1β might play a role in regulating neutrophil mobilization from the BM.

To test whether the increase in IL-6 upon *C. albicans* colonization was a result of local expansion of IL-6–producing cells, we harvested the blood and BM cells from mock-treated or *C. albicans*–colonized mice and quantified IL-6$^+$ cells by flow cytometry. *C. albicans* colonization increased the proportion of IL-6$^+$ cells locally in the BM and not in the blood (Fig. 4H). IL-6$^+$ myeloid cells (CD45$^+$ B220$^-$CD3e$^-$CD19$^+$) increased in *C. albicans*–colonized mice and were the main source of IL-6 in the BM (Fig. 4I and fig. S5A). To further define the cell types that contributed to *Il6* expression, we performed single-cell RNA sequencing (scRNA-seq) on BM cells isolated from mock-treated and *C. albicans*–colonized mice. We used unsupervised dimensionality reduction analysis combined with unbiased cell type recognition using the ImmGenData open-source (expression) reference database to identify various hematopoietic populations consisting of murine progenitors, neutrophils, monocytes, plasmacytoid dendritic cells, macrophages, Mast/basophils, and B and T lymphocytes (fig. S5B). The *Il6*-expressing cluster was enriched for *Fcer1a* (Fc epsilon RI), *Cd200r3* (CD200R3), and *Mcpt8* (Mast cell protease 8) expression, identifying the cells as a mast/basophil subset (Fig. 4J and fig. S5C). Analysis of several other detectable cytokines indicated that the *Il6* expression pattern was distinct in our dataset. For instance, *Il1b* and *Il18* expression was mainly detected in neutrophils and macrophages, respectively (Fig. 4J). Consistent with previous studies showing that human and mouse HSC/progenitors respond to IL-6 (*61*, *62*), expression of genes encoding the IL-6R complex, *Il6ra* and *gp130* (*Il6st*), was detected in the "progenitor" cluster, and their expression was up-regulated in response to *C. albicans* colonization (fig. S5, D and E). These results indicate that granulopoiesis induced by *C. albicans* colonization is associated with the expansion of IL-6$^+$ myeloid cells, in particular mast/basophils, in the BM.

Hypha-associated candidalysin promotes granulopoiesis

C. albicans morphogenesis and associated virulence factors play important roles in the host immune response and commensal fitness (*63*–*65*). Histological analyses of *C. albicans* in mouse intestines with periodic acid–Schiff (PAS) staining, which stains polysaccharides on the surface of *C. albicans*, showed plenty of oval-shaped cells that indicated the typical yeast morphology (Fig. 5A). Elongated morphological structures were also visible. Similar results were obtained by immunofluorescence microscopy (Fig. 5B). A large quantity of yeast-like *C. albicans* were detected in the mucus layer close to the intestinal epithelium, but excluded from the tissue, suggesting lack of invasion.

The transcription factors EFG1 and FLO8 are essential for filamentous growth and regulate the expression of virulence factors in response to environmental cues, such as temperature, pH, or nutrients (*66*–*69*). Thus, to examine whether these morphogenic regulators of *C. albicans* were required for promoting granulopoiesis in the BM, we compared mice colonized with wild-type versus *efg1*Δ/Δ and *flo8*Δ/Δ mutant *C. albicans*. Although these yeast-locked mutants displayed similar burden in stool as the isogenic wild-type control, both *efg1*Δ/Δ and *flo8*Δ/Δ *C. albicans* lost the ability to induce MPP3 in the BM and neutrophils in the blood (Fig. 5, C and D). We confirmed that structures indicative of hyphal morphology were absent in mice colonized by *flo8*Δ/Δ *C. albicans* (Fig. 5E). Among the most characterized factors that are up-regulated during hyphal formation in *C. albicans* is the immunogenic mycotoxin candidalysin (*70*). The candidalysin-deficient (*ece1*Δ/Δ) mutant did not increase granulocyte and neutrophil levels compared with mock-treated mice. Furthermore, *ece1*Δ/Δ *C. albicans* induced significantly reduced MPPs and MPP3 compared with wild-type *C. albicans*. Fungal burdens in stools of wild-type and *ece1*Δ/Δ *C. albicans* were comparable (Fig. 5, F to H). In addition, the proportion of newly released neutrophils (CD62L^{hi}CXCR4^{lo}) in mice colonized by these *C. albicans* mutants was similar to control uninoculated mice (Fig. 5I). These findings indicate that the hypha-associated virulence factor ECE1 promotes granulopoiesis.

Fungal colonization enhances protection against gram-positive bacterial infections

We next asked whether the response to fungal colonization of the gut leads to altered susceptibility to bloodstream infection by *S. aureus*, a bacterial pathogen sensitive to granulocytes (*71*). Consistent with this possibility, laboratory mice colonized with *C. albicans*

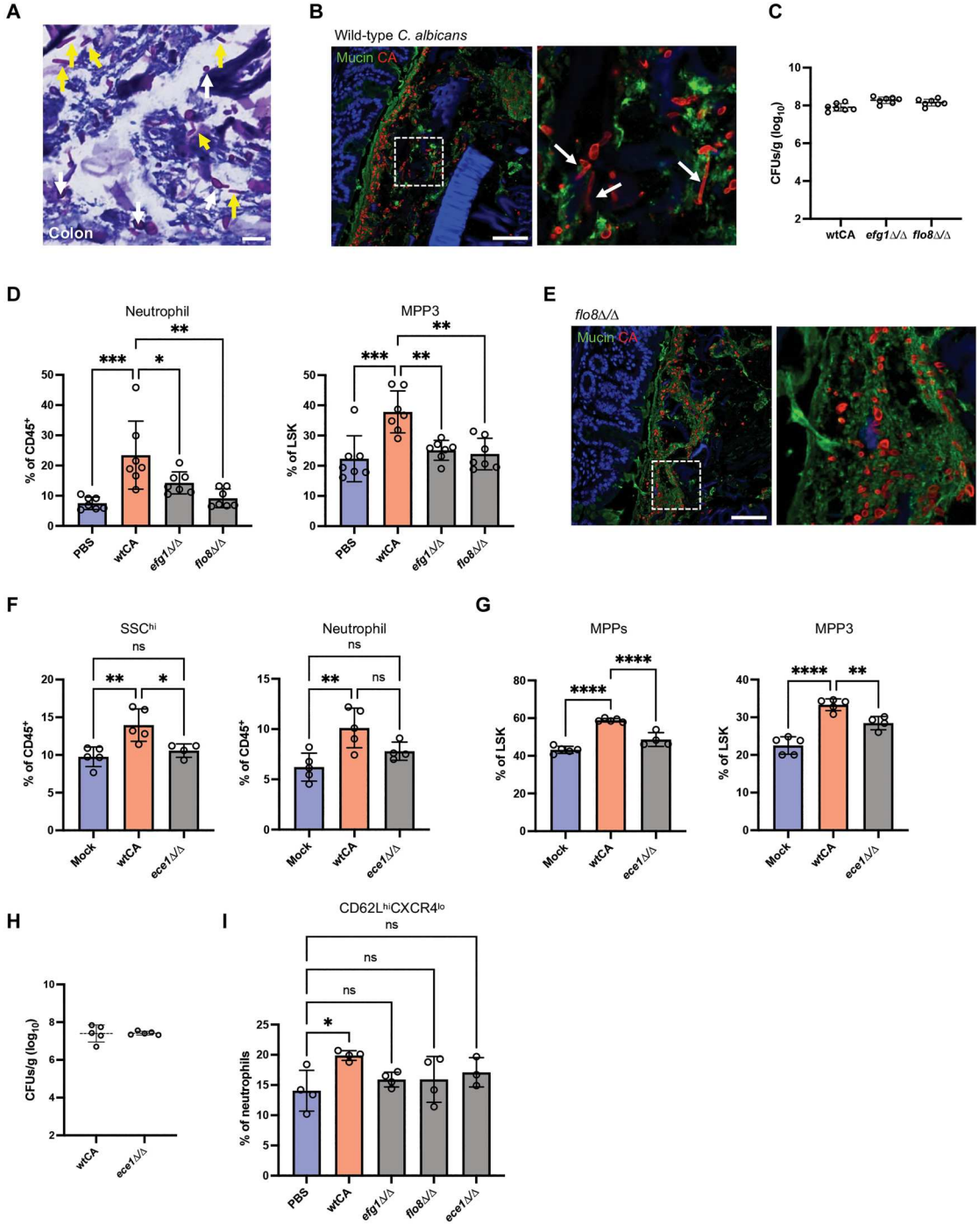

Fig. 5. Candidalysin promotes granulopoiesis. (**A**) PAS-stained colonic section from *C. albicans*–colonized antibiotic-treated mice. White and yellow arrows indicate yeast and hyphal structures, respectively. Scale bar, 10 μm. (**B**) Confocal images of wild-type *C. albicans*–colonized colon sections immunostained with anti-candida antibody and counterstained with FITC-lectins mixture. Region of interest is magnified in right. Arrows indicate the hyphal structure. Scale bar, 100 μm. (**C**) Fungal CFUs in feces from antibiotic-treated mice 21 days after inoculation with wild-type *C. albicans* and yeast-locked mutants. (**D**) Frequency of neutrophils in the peripheral blood and MPP3 in the BM on day 21 after wild-type and mutant (*efg1*Δ/Δ and *flo8*Δ/Δ) *C. albicans* inoculation. $n = 7$ mice per group. (**E**) Confocal images of colon sections from mice colonized with the *FLO8* deletion mutant immunostained with anti-candida antibody and counterstained with FITC-lectins mixture. Region of interest is magnified in right. Scale bar, 100 μm. (**F**) Frequency of SSC^{hi} granulocytes and neutrophils in the peripheral blood on day 21 after wild-type and mutant (*ece1*Δ/Δ) *C. albicans* inoculation. (**G**) Frequency of MPPs and MPP3 in the BM on day 21 after wild-type and mutant (*ece1*Δ/Δ) *C. albicans* inoculation. $n = 5$ PBS control, $n = 5$ *wtCA*-colonized mice, and $n = 4$ mutant (*ece1*Δ/Δ) *CA*–colonized mice. (**H**) Fungal CFUs in feces from antibiotic-treated mice 21 days after inoculation with wild-type and *ece1*Δ/Δ *C. albicans*. (**I**) Frequency of fresh neutrophils ($CD62L^{hi}CXCR4^{lo}$) in the peripheral blood on day 21 after wild-type and mutant *C. albicans* inoculation. Dots in bar graphs correspond to individual mice. Mean and SD are shown. $^{*}P < 0.05$, $^{**}P < 0.01$, and $^{****}P < 0.0001$ by ordinary one-way ANOVA with Holm-Šidák multiple comparisons test.

for 3 weeks displayed substantially enhanced survival after intravenous infection by methicillin-resistant *S. aureus* (MRSA) strain USA300 (Fig. 6A). Our experiments examining cell surface markers suggest neutrophils from *C. albicans*–colonized mice were qualitatively different. To examine phagocytic capacity ex vivo, we cocultured neutrophils and green fluorescent protein (GFP)–labeled *S. aureus* incubated with serum to allow for opsonization and used heat-treated serum in which complement proteins were inactivated as a control. Neutrophils isolated from *C. albicans*–colonized mice exhibited enhanced phagocytosis of opsonized *S. aureus* (Fig. 6, B and C), indicating that fungal colonization boosted both quantity and function of neutrophils. In addition, we found *S. aureus* burden in various organs were decreased in *C. albicans*–colonized mice compared with control mice, especially in the blood and lungs (fig. S6A). Fungal colonization has been shown to contribute to expansion of protective T_H17 cells and induce an antifungal immunoglobulin G (IgG) response against pathogens (*30*, *72*). To rule out potential cross-reactivity of lymphocytes between microbes, recombination activating gene 1 (RAG-1)–deficient mice, lacking mature B and T lymphocytes, were challenged with *S. aureus* after 3 weeks of *C. albicans* colonization. *C. albicans*–colonized RAG-1–deficient mice, which we confirmed showed comparable fungal burden in the stool as other experiments, displayed improved survival during *S. aureus* infection compared with the noncolonized control *Rag-1*$^{-/-}$ mice (Fig. 6D and fig. S6B). In contrast, depletion of neutrophils with anti-Ly6G antibodies abrogated the protection conferred by *C. albicans* colonization (Fig. 6E). Although the degree of survival among control groups was variable, which may be inherent to sepsis models (*73*), these results show that *C. albicans* consistently protected the host across experiments when neutrophils are present. Also, *C. albicans* mutants that are unable to induce MPP3 in the BM and neutrophils in the blood, *efg1*Δ/Δ and *flo8*Δ/Δ, completely lost the ability to protect the mice from *S. aureus* infection (Fig. 6F and fig. S6C). Last, the protection induced by fungal colonization was not specific for *S. aureus* infection; *C. albicans*–colonized mice also improved survival after intraperitoneal or intranasal infection with *Streptococcus pneumoniae* (Fig. 6G and fig. S6D). Together, these results show that immune alterations associated with *C. albicans* colonization of the gut enhance protection against gram-positive bacterial pathogens.

Intestinal fungal colonization mediates longer-lasting protection compared with innate immune training

Our finding that *C. albicans* improves survival of *Rag1*$^{-/-}$ mice in a manner dependent on neutrophils during *S. aureus* infection indicates that fungal colonization mediates protection by enhancing innate immunity. β-Glucan, a potent stimulant of trained immunity, reprograms the immune cells epigenetically or functionally to enhance host responses (*74*). Trained immunity stimulated by β-glucan induces impressive broad-spectrum protective responses against secondary infections (*38*, *39*, *75*). Although our results showed that granulopoiesis wanes over time in transiently stimulated mice compared with persistent fungal colonization (Fig. 3), BM cells from mice injected with β-glucan display an enhanced ability to reinitiate myeloid cell differentiation upon rechallenge, indicating that some immune changes are sustained in this model (*76*). Because persistent exposure to fungi maintains granulocyte levels in the blood (Fig. 3), we investigated whether fungal colonization would afford greater protection from a bacterial infection compared with the previously described β-glucan–induced trained immunity that involves a recall response. To test our hypothesis, we compared laboratory mice colonized by *C. albicans* through oral inoculation and mice injected intraperitoneally with β-glucan that received a secondary challenge with *S. aureus* either at 7 days or 3 weeks after colonization or injection (Fig. 7A). β-Glucan–induced circulating neutrophil levels return to baseline at these time points (Fig. 3D); therefore, any protection can be attributed to innate immune memory. At the 7-day time point, *C. albicans* colonization and β-glucan injection led to a similar degree of enhanced protection compared with control mice (Fig. 7B). In contrast, at 3 weeks after treatment, protection against *S. aureus* induced by β-glucan was absent, yet fungal colonization was capable of sustaining enhanced immunity (Fig. 7, C and D). Consistent with this finding, intestinal *C. albicans* protected *Dectin-1*$^{-/-}$ mice from *S. aureus* infection (Fig. 7E). Overall, fungal gut colonization led to sustained changes to the host immune system that mediated greater and prolonged protection against pathogenic infection.

DISCUSSION

Granulocyte abundance and function is one of the most recognized differences between humans and mice. Granulocytes make up only 5 to 10% of leukocytes in mouse blood but 50 to 70% in humans. Our results indicate that the environment, specifically sustained stimulation by intestinal fungi, may account for at least part of this difference by regulating granulopoiesis in the BM. A comprehensive study showed that gut fungal communities in SPF C57BL/6J laboratory mice vary across vendors and are shaped by the environment, bacterial communities, and diet (*77*). Although the degree of fungal colonization and community composition is likely facility dependent, most studies do not report the retrieval of fungi from SPF mice through culturing techniques. Therefore, fungal burden may be low in many conventional animal facilities, as we previously observed (*16*). In addition to our report, another group showed that wild mice have significantly higher relative abundance of intestinal fungi (*13*). Thus, a certain level of fungal colonization may be the norm for free-living mammals. Consistent with this idea, the effect of rewilding on granulocytes and acquisition of intestinal fungi was reproducible across years. However, in contrast to the carefully controlled laboratory experiments in which mice are inoculated with a defined amount of *C. albicans*, we consistently observed greater variance in granulocyte numbers among rewilded mice. We previously showed a positive correlation between granulocyte and fungal abundance, and the specific association between neutrophils and fungal burden was confirmed here. Considering that humans display interindividual differences in fungal microbiota, including the presence and abundance of pro-inflammatory *C. albicans* strains (*78*, *79*), interindividual variation in fungal exposures and immune traits may be another aspect of human biology that is captured in the outdoor mouse enclosure (*80*).

We note that fungal colonization of mice falls short of fully recapitulating the relative proportion of various leukocytes observed in humans and that many environmental and species-intrinsic factors likely contribute to deficiencies in the laboratory mouse model for studying human immunity. Exposure to pathogens, as opposed to commensals, may be particularly important for the maturation of certain aspects of the adaptive immune system (*9*, *12*). We

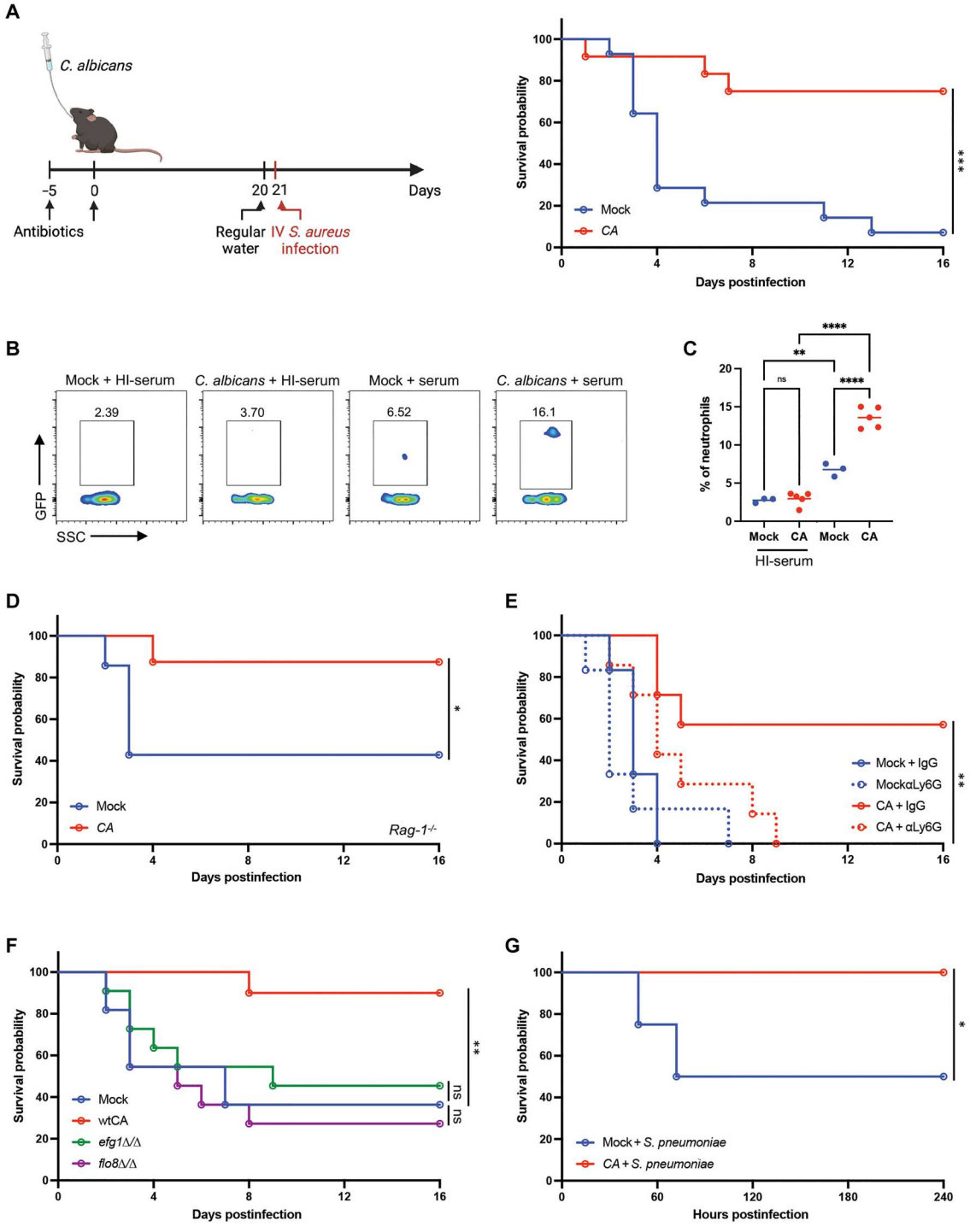

Fig. 6. Intestinal colonization by *C. albicans* protects against gram-positive bacterial infections. (**A**) Survival after intravenous (i.v.) injection of *S. aureus* on day 21 after PBS (mock, $n = 14$) or *C. albicans* ($n = 12$) inoculation. Antibiotics-containing water was swapped with regular water 24 hours before *S. aureus* infection. Three independent repeats. (**B**) Representative flow cytometry plots of neutrophils isolated from the BM of mock and *C. albicans*–colonized mice incubated with GFP-labeled *S. aureus* together with untreated or heat-inactivated (HI) mouse serum for 20 min at an MOI of 25. (**C**) Quantification of frequency of GFP^+ neutrophils from (B). $n = 3$ mock and $n = 5$ *C. albicans*–colonized mice. (**D**) Survival of *Rag1*$^{-/-}$ knockout mice infected with *S. aureus* on day 21 after PBS ($n = 7$) or *C. albicans* ($n = 8$) inoculation. Two independent repeats. (**E**) Survival of mice infected with *S. aureus* on day 21 after PBS or *C. albicans* inoculation and treated with anti-Ly6G or IgG isotype control antibodies on days −1, 1, 3, 5, and 7 days after infection. $n = 7$ mice per group. (**F**) Survival of mice infected with *S. aureus* on day 21 after inoculation with PBS, wild-type, or mutant *C. albicans* (*efg1*Δ/Δ and *flo8D/flo8*Δ/Δ). $n = 22$ mice per group. Two independent repeats. (**G**) Survival of mice injected intraperitoneally with *S. pneumoniae* on day 21 after PBS or *C. albicans* inoculation. $n = 12$ mice per group. Dots in bar graphs correspond to individual mice. Mean and SD are shown. $^*P < 0.05$, $^{**}P < 0.01$, $^{***}P < 0.001$, and $^{****}P < 0.0001$ by ordinary one-way ANOVA with Holm-Šidák multiple comparisons test (C). (A and D to G) log-rank Mantel-Cox test.

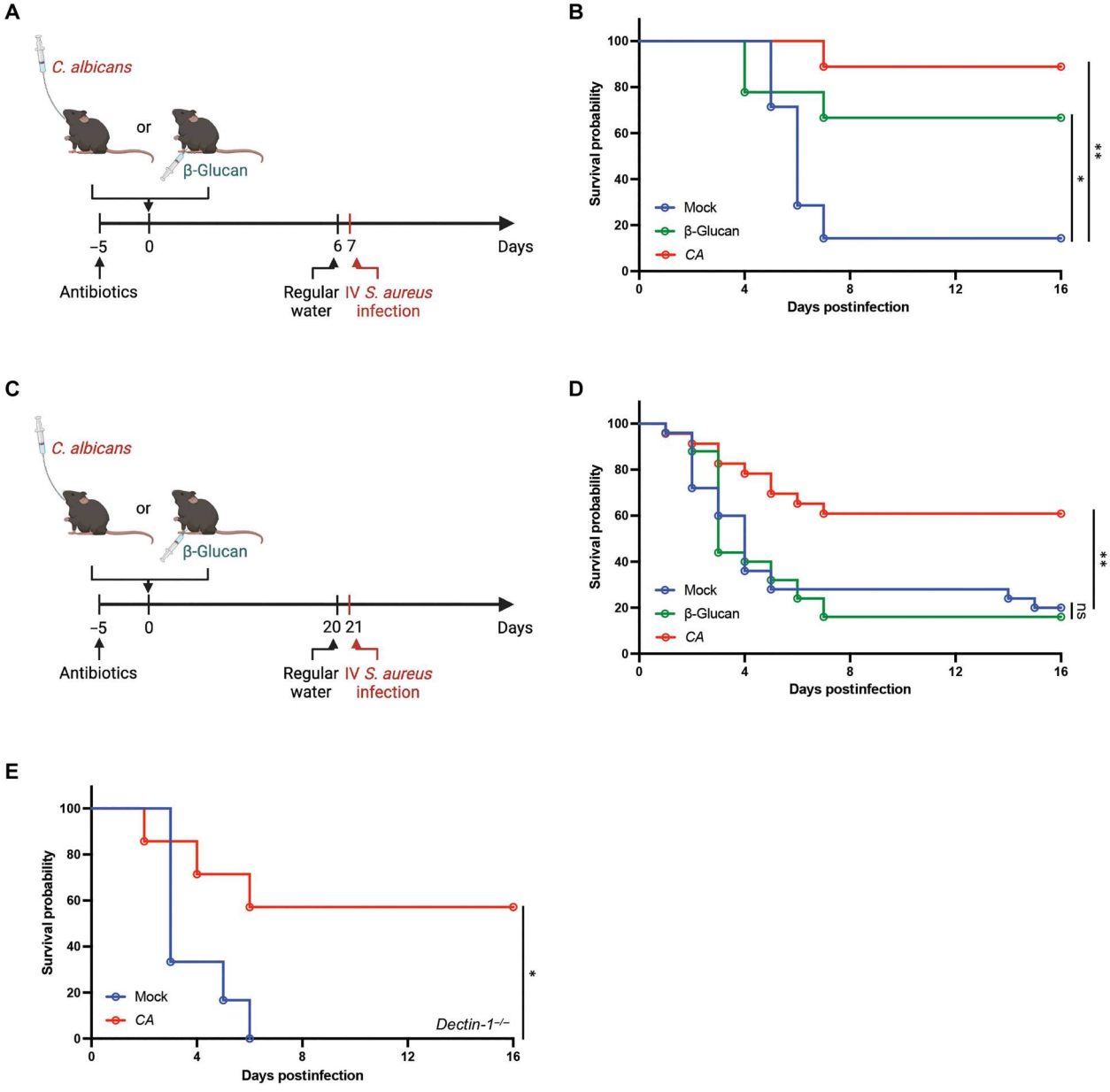

Fig. 7. Intestinal *C. albicans* colonization mediates longer-lasting protection from *S. aureus* compared with β-glucan stimulation. (**A**) Schematic depicting experimental procedure in (B). Antibiotic-treated mice were orally inoculated with PBS (mock) ($n = 7$) or *C. albicans* ($n = 9$) or intraperitoneally injected with β-glucan (1 mg) ($n = 9$). Antibiotics-containing water was swapped with regular water on day 6 and mice were injected i.v. with *S. aureus* on day 7. (**B**) Survival of mice infected with *S. aureus* on day 7 after inoculation with *C. albicans* or β-glucan. (**C**) Schematic depicting experimental procedure in (D) and (E). Similar to (A) except mice were injected i.v. with *S. aureus* on day 21. (**D**) Survival of mice infected with *S. aureus* on day 21 after inoculation with *C. albicans* or β-glucan. $n = 25$ mice per group. Two independent repeats. (**E**) Survival of *Dectin-1*$^{-/-}$ mice infected with *S. aureus* on day 21 after inoculation with *C. albicans* or β-glucan. $n = 7$ mice per group. *$P < 0.05$ and **$P < 0.01$ by log-rank Mantel-Cox test (B, D, and E).

also note that the pronounced eosinophil expansion observed in rewilded mice was not reproduced with *C. albicans* inoculation. Fungi isolated from rewilded mice better recapitulated the increase in peripheral eosinophils, suggesting that even among fungi, the exact host response to intestinal exposure is dependent on the fungal species and strains.

Mechanistic insight came from our finding that transcription factors controlling hyphal morphogenesis were necessary for enhanced granulopoiesis, leading us to identify candidalysin as an essential factor in this host response. Candidalysin induces membrane damage in target cells to evoke cytokines including IL-6 and IL-1β (*70*). Other fungi produce mycotoxins, which may explain why exposure to fungi in the outdoor enclosure induces similar (but not identical) outcomes as colonization by *C. albicans*. In addition, fungal sensors such as dectin-1 were dispensable, further supporting a model in which granulopoiesis is driven by

subtle cellular damage by candidalysin, although our findings do not rule out a role for orthogonal pathways that are triggered by yeast-to-hyphae transition. Multiple pathogen sensors act in an overlapping or redundant manner during innate immune memory and T_H17 response elicited by intravenous injection and gut colonization with *C. albicans*, respectively (*81*, *82*), and although β-glucan has received the bulk of attention, a recent study showed that fungal mannans travel through the lymph from the periphery to stimulate a potent CARD9-independent immune response (*83*).

The functional consequences of the enhanced granulopoiesis in response to fungal colonization were profound. *C. albicans* can exacerbate the adverse consequences of *S. aureus* infection when found together, such as through fungal hypha-associated adhesions factors that promote mixed biofilm formation (*84*–*86*). We found that when colonization was restricted to the gut, even after a month after the initial inoculation, *C. albicans* continued to sustain high levels of peripheral neutrophils and substantially protected against bacterial infection. This observation motivated us to compare gut colonization with transient stimulation of antifungal defense, an established trigger of granulopoiesis. Similar to the short-term response to systemic infection by *C. albicans* (*87*), we found that neutrophils expanded and declined rapidly in the periphery in a 3-day span after β-glucan injection. Despite this return to baseline, we reproduced observations in the literature by showing that β-glucan injection provided enhanced protection through trained immunity when the bacterial challenge occurred a week after priming. However, β-glucan injection failed to confer protection at 1 month after priming. The recall response is potentially slower or less efficient at later time points when innate immune memory wanes, whereas mice experiencing persistent fungal colonization benefit from constitutively high levels of circulating fresh neutrophils. It is also possible that reprogramming leads to a qualitatively different response that relies on monocytes and macrophages more so than neutrophils (*38*, *39*). In addition, the fungal determinants of short- versus long-term effects on the host are distinct. When delivered intravenously, *C. albicans* defective in hypha-associated gene expression was able to confer short-term protection from subsequent infectious disease challenges similar to β-glucan injection (*27*). In contrast, we found that protection conferred by gut colonization was dependent on the hypha-associated gene expression program.

In conclusion, our results indicate that fungal colonization continually promotes granulopoiesis and neutrophil expansion through a mechanism distinct from infection-induced emergency granulopoiesis or trained immunity. The sustained immune activation offers prolonged protection against bloodstream pathogens. Recent evidence highlights a previously unappreciated heterogeneity of neutrophils, which may be key for their function during infectious and chronic diseases, such as cardiovascular inflammation and cancer (*88*–*90*). The newly produced neutrophils induced by fungi may carry distinct characteristics that are missing in laboratory mice. Given that humans and free-living mammals are exposed to fungi from the environment constantly, introducing fungi into laboratory mice is likely to better recapitulate certain aspects of mammalian biology.

MATERIALS AND METHODS

Study design

The aim of this study was to reveal how intestinal fungi modulate HSCs and progenitors, in particular myeloid-biased MPP3, leading to increased granulopoiesis and circulating neutrophils in the blood. In addition to rewilding in which laboratory mice experience a seminatural environment through release into an outdoor enclosure facility, we used human commensal fungi, *C. albicans*, in the laboratory to recapitulate the expansion of granulocytes. MPPs and MPP3 in BM were analyzed by flow cytometry to determine the levels of granulopoiesis. β-glucan injection, which mimics fungal infection, was used to compare to fungal colonization in the gut. Last, we assessed their protective potential against gram-positive bacteria. Mice were randomly assigned to individual groups and analyzed without excluding outliers. The rewilding procedure and facility is described in detail below. All laboratory experiments were performed at least two times independently. The number of mice and statistics used in the studies are included in the figure legends.

Mice and wild enclosure

All mouse lines were on a C57BL/6J background and bred onsite in an MNV/*Helicobacter*-free SPF facility at NYU Grossman School of Medicine. C57BL/6J [wild type (WT)], *Dectin-1*$^{-/-}$ (*Clec7a*$^{-/-}$), and *Card9*$^{-/-}$ mice were initially purchased from the Jackson Laboratory. Rorc(γt)–enhanced GFP (*Rorc*$^{-/-}$) mice were obtained from D. Littman, NYU Grossman School of Medicine. All animal work was approved by NYU Langone Institutional Animal Care and Use Committee (IACUC; #IA16-0087 and #IA16-00864). For experiments performed within the institutional SPF facility that involved inoculation with microbes, 6- to 10-week-old mice of both sexes were used and compared with control-treated littermates. Littermates of mice used for rewilding experiments were generated from multiple breeding pairs and randomly assigned to either remain in the institutional vivarium (laboratory mice) or released into the outdoor enclosures (rewilded mice) to control for the microbiota at the onset of the experiment. Outdoor enclosures were previously described (*15*, *16*) and the protocols for releasing the laboratory mice into the outdoor enclosure facility were approved by Princeton IACUC (#1982-17).

The Stony Ford outdoor enclosure was previously described (*15*, *16*). In brief, the enclosure consists of wedges, each measuring about 180 m^2 and fenced by 1.5-m high zinced iron walls that are buried >80 cm deep and topped with electrical fencing to keep out terrestrial predators. A straw-filled shed is provided in each enclosure, along with two watering stations and a feeding station, so that the same mouse chow used in the laboratory (PicoLab Rodent Diet 20) was provided ad libitum to all mice. Mice outdoors, however, also had access to food sources found within the enclosures, including berries, seeds, and insects. Twelve WT, 10 *Dectin-1*$^{-/-}$, and eight *Card9*$^{-/-}$ female laboratory mice were housed in the enclosure for 6 to 7 weeks. Nine WT, eight *Dectin-1*$^{-/-}$, and eight *Card9*$^{-/-}$ matched littermates were maintained in the institutional vivarium for comparison. Longworth traps baited with chow were used to catch mice after release. All rewilded mice were caught in the final trapping for terminal analyses and all laboratory control mice were recovered. Euthanasia was performed by CO_2 asphyxiation, and blood, femur, and intestinal tissue were harvested. The

presence of macroscopic parasites in multiple organs and microscopic parasites by histology was analyzed to confirm that the mice in the outdoor enclosure were free from parasite infection in rewilding experiments.

Construction of *C. albicans* strains

Yeast extract, peptone, and dextrose (YPD) medium was prepared as previously described (*91*). Synthetic complete medium (SCM) medium was prepared as for SCD medium (*91*) except 2% maltose was included in place of dextrose. YPD supplemented with nourseothricin (200 μg/ml; Werner BioAgents, Jena, Germany) was used to select for nourseothricin-resistant (NAT^R) strains.

To generate an *efg1*Δ/Δ strain, pRB721 (*25*) was digested with Apa I and Sac I and transformed into SC5314 strain to generate NAT^R *EFG1* heterozygotes. Integration was checked by polymerase chain reaction (PCR) using oligos 2284/4438 and 2286/4439. The *SAT1* marker was recycled by growing on SCM medium and a second round of transformation performed to delete the remaining *EFG1* allele using pRB721 to create a NAT^R *efg1* null. Correct integration was confirmed and the absence of the *EFG1* gene established by PCR using oligos 819/828. The *SAT1* marker was recycled by growth on maltose to generate the NAT-sensitive (NAT^s) *efg1* null strain CAY10195.

To delete the *FLO8* gene, a pSFS-*FLO8* knockout plasmid (pRB989) was first constructed. Oligos 4988/4989 and 4990/4991 were used to PCR amplify 5′ and 3′ untranslated regions of the *FLO8* gene from the SC5314 strain background. These two fragments were cloned into pSFS2A (*92*) using Apa I/Xho I and Sac I/Sac II sites, respectively. To create a *flo8*Δ/Δ strain, pRB989 was cut by Apa I/Sac I and transformed into SC5314, generating a *FLO8*/*flo8*Δ strain. PCR was performed to check integration using oligos 4982/4438 and 5076/4439. After recycling the *SAT1* marker by growth on SCM, pRB989 plasmid was again digested by Apa I/Sac I to perform the second round of transformation, resulting in a *flo8*/*flo8* mutant. PCR checks were performed using oligos 4982/4438, 5076/4439, and 5200/4986. The NAT^R marker was recycled by growth on SCM to generate the NAT^S *flo8*Δ/Δ strain CAY10993.

To generate SC5314 *ece1*Δ/Δ, oligos 4248/4249 were used to amplify the ARG4 and HIS1 cassettes from a published *ece1*Δ/Δ and transformed into strain SN95 (*93*). Cells were grown on SC medium without arginine to select for transformants. Junction PCR checks were performed using oligos 4252/4287 and 4286/4253. The transformation was repeated to delete the second *ECE1* allele and transformants grown on SC medium lack of histidine and arginine. Transformants were PCR checked using oligos 4250/4251 for open reading frame, 4252/4289 for the 5′ junction, and 4288/4253 for the 3′ junction. To generate the NAT^R version of ece1Δ/Δ, the pDis3 plasmid was used to integrate into the NEUT5L locus as described previously (*94*). The plasmid was linearized by NgoMIV and transformed into ece1Δ/Δ to create NATR CAY11507. PCR checks were performed using oligos 3055/3056.

C. albicans inoculation

A single colony of wild-type or mutant *C. albicans* was cultured in 5 ml of Sabouraud dextrose (SD) media with chloramphenicol (25 μg/ml; Sigma-Aldrich) at 30°C for 16 hours. Cells were pelleted at 1000*g* for 5 min and washed with 1× sterile phosphate-buffered saline (PBS) three times. *C. albicans* then was resuspended in 2 ml of 1× PBS. Germ-free or antibiotics-treated (1 g of ampicillin and 0.5 g of streptomycin in 1 liter of sterilized water) mice were orally gavaged with 150 μl of *C. albicans* [~2×10^7 colony-forming units (CFUs) per mouse] using plastic feeding tubes (Instech Laboratories). After the inoculation of *C. albicans*, feces and organs were collected and analyzed at different time points according to the experiments. For depletion of colonized *C. albicans*, germ-free mice were supplemented with fluconazole (0.5 g/liter) in drinking water for 2 weeks. The fecal pellets were homogenized in PBS and serial dilutions of fecal samples were plated on SD plates to determine the fungal CFU of wild-type and mutant strains.

Isolation of mouse LP cells

Lamina propria (LP) cells were harvested as previously described (*95*). In brief, small intestine and colonic tissues were cut open and washed with PBS, and fat was removed. The tissues were incubated first with 20 ml of Hank's balanced salt solution (HBSS; Gibco) with 2% Hepes, 1% sodium pyruvate, 5 mM EDTA, and 1 mM DL-dithiothreitol (Sigma-Aldrich) for 15 min at 37°C with 220 rpm and then with new 20 ml of HBSS with 2% Hepes, 1% sodium pyruvate, and 5 mM EDTA for 10 min at 37°C with 220 rpm. The tissue bits were washed with HBSS, minced, and then enzymatically digested with collagenase (0.5 mg/ml; Sigma-Aldrich) and deoxyribonuclease I (0.01 mg/ml, Sigma-Aldrich) for 30 min at 37°C with 200 rpm. Digested solutions were passed through 70-μm nylon mesh (ELKO Filtering) and isolated cells were resuspended in 40% Percoll (Sigma-Aldrich), layered onto 80% Percoll, and centrifuged without brake at room temperature at 2200 rpm for 22 min. Cells were recovered from the interphase and washed with RPMI1640 (Corning) containing 10% fetal bovine serum (FBS; Peak Serum) and used as LP cells.

Flow cytometry analysis

Whole blood was collected through cardiac puncture from mice and kept in a heparin containing tube on ice. Femur was isolated from the surrounding tissue and cleaned with a surgical scalpel and paper towels to remove surrounding muscle and connective tissue. The BM content was flushed out and BM fluid was collected and kept at −80°C until all samples were collected and analyzed together. A total of 200 μl of blood sample and all BM cells were resuspended in 5 and 2.5 ml of 1× red blood cell lysis buffer (BioLegend, CA), respectively, for 10 min to lyse the red blood cells. After two washes with cold PBS, BM and blood cells were signalized through 35-μm strainer with ice-cold fluorescence-activated cell sorting (FACS) buffer (PBS, 2% FBS, and 1 mM EDTA). Single-cell suspensions of BM cells in FACS buffer was counted using an automatic cell counter with trypan blue (Countess 3, Thermo Fisher Scientific). The staining antibodies for flow cytometry were purchased from Thermo Fisher Scientific, BioLegend, or BD Biosciences. For cell surface staining, cells were incubated with antibodies at 4°C for 20 min and fixed for 20 min at room temperature. All antibodies were used at a dilution of 1:100 unless otherwise noted. For cell surface phenotype analysis, a mouse lineage antibody cocktail (BD Biosciences, 1:10), anti–Siglec-F (E50-2440), anti-B220 (RA3-6B2), anti-NK1.1 (PK136), anti-TCRβ (H57-597), anti-CD3ε (145-2C11), anti-CXCR4 (L276F12), anti-Ly6G (1A8), anti-CD62L (MEL-14), anti-CD45 (30-F11), anti-CD4 (GK1.5), anti-CD8a (53-6.7), anti-CD127 (A7R34), anti-Ly6C (AL-21), anti-CD11b (M1/70), anti-Flt3 (CD135) (A2F10, 1:50), anti–Sca-1 (Ly6A/E)

(E13-16L7), anti-CD150 (TC15-12F12.2, 1:50), anti-CD48 (HM48-1), anti–c-Kit (CD117) (2B8), anti-CD115 (AFS98), anti-GR1 (RB6-8C5), and anti-CXCR2 (5E8/CXCR2) were used. For cytokine staining, cell was plated in RPMI1640 and stimulated with 1× cell stimulation cocktail (plus transport inhibitors) (eBiosciecne) for 4 hours at 37°C. For intracellular staining of cytokines, cells were permeabilized with intracellular staining permeabilization wash buffer (BioLegend) at room temperature for 20 min in the presence of antibodies. For intracellular staining of the transcription factor, cells were permeabilized with the Foxp3/transcription factor staining buffer set (BD Biosciences) at room temperature for 45 min in the presence of antibodies. The following antibodies for intracellular staining were used: anti–IL-6 (MP5-20F3), anti–IL-17A (TC11-18H10.1), anti-RORγt (562894), and anti-GATA3 (L50-823). Dead cells were excluded using Invitrogen Fixable Blue Dead Cell Stain Kit (Thermo Fisher Scientific). Flow cytometry data were acquired on the ZE5 cell analyzer (Bio-Rad) and analyzed on FlowJo version 10.8.1.

Cytokine measurements

To collect BM extracellular fluid, BM content in a femoral bone was harvested by centrifugation at 13,000 rpm for 15 s and resuspended with ice-cold PBS (50 μl). The supernatant then was collected after pelleting cells by centrifugation at 350*g* for 5 min at 4°C. Cytokines in supernatants were measured using the mouse IL-6 and IL-1 β/IL-1 F2 DuoSet enzyme-linked immunosorbent assay (R&D systems) according to the manufacturer′s instructions.

Cell depletions and cytokine neutralization

To deplete immune cells or neutralize cytokines, antibiotics-treated mice were injected intraperitoneally 1 day before and every other day after *C. albicans* inoculation until 7 days after inoculation with 200 μg of InVivoMab anti–IL-6R (clone 15A7; BioXCell), 100 μg of InVivoMab anti-Ly6G (clone 1A8; BioXCell), InVivoMab anti-CD4 (clone GK1.5, BioXCell), InVivoMab IL-1α (clone ALF-161; BioXCell), InVivoMab IL-1β (clone B122; BioXCell), and InVivoMab GM-CSF (clone MP1-22E9; BioXCell) in 100 μl of PBS, respectively. Mock or *C. albicans* control mice received equal volumes of PBS or equal amounts of InVivoMab rat IgG isotope control antibodies (clone LTF-2; BioXCell). At day 7, mice were euthanized and organs were harvested for further analysis.

Isolation of primary mouse neutrophils and serum

Adult mice were euthanized and whole blood from cardiac puncture was then collected in heparin containing tubes. Designated serum from supernatant was collected after centrifuging at 2000 rpm for 5 min and stored at 4°C until future use. The hind limbs of each mouse were washed with an excess of 70% EtOH. Skin was separated until the femurs were exposed, allowing for removal at the proximal hip and distal knee joint. Excess tissue and muscle were removed with paper towels, and clean bones were placed in fresh 1× PBS on ice. The BM cells were flushed out, washed with FACS buffer, and filtered through a 70-μm cell strainer. Single-cell suspensions of whole blood cells and BM cells in FACS buffer were counted using an automatic cell counter with trypan blue and placed on ice. Neutrophil enrichment was performed using EasySep Mouse Neutrophil Enrichment Kit (Stem Cell Technology) following the manufacturer′s instructions.

Neutrophil phagocytosis assay

GFP–*S. aureus* (USA300) strain was streaked to single colonies on a tryptic soy agar (TSA) plate. Single colonies were inoculated in tryptic soy broth (TSB) broth for overnight culture and then subsequently subcultured 1:100 for 3 hours in TSB at 37°C with shaking. Subcultures were centrifugated at 4000 rpm and resuspended to final infection concentration (10^8 cells per ml) in cold PBS. Bacteria was opsonized by mixing 1:1 with fresh mouse serum or heat-inactivated control at 37°C on rotary board for 45 min. Neutrophils from whole blood and BM were isolated as described above. Neutrophils were seeded at 10^5 cells per well in RPMI + 10% FBS containing 96-well plates. Plates were allowed to rest for 10 min on rotary board at 37°C, opsonized bacteria were then added at a multiplicity of infection (MOI) of 20, and the place was returned to the incubator. After 20 min, the plate was immediately placed on ice for 3 min and extensively washed twice with cold PBS. Neutrophils were stained for live/dead with blue reactive dye and neutrophil cell surface markers as previously described.

Imaging of *C. albicans* in the murine intestine

At 21 days after inoculation of wild-type *C. albicans* or mutant strains, mice were euthanized, and segments with feces of the ileum and colon were fixed in the Methanol-Carnoy′s solution [60% (v/v) dry methanol, 30% (v/v) chloroform, and 10% (v/v) glacial acetic acid] for 48 hours at room temperature. Fixed tissues were processed twice in 100% ethanol for 20 min and twice in xylene for 15 min, and embedded in paraffin wax. The sections of the tissues were first dewaxed with an initial incubation at 60°C for 10 min and two additional incubations in xylene substitute solution. The samples were rehydrated in the solutions with a descending ethanol gradient (100, 95, 70, and 50%) for 3 min (two times each) and followed by two washes in water. The sections were then ready for PAS or immunofluorescence staining. For imaging of fungi, after one wash of 0.1% Triton X-100/PBS for 5 min, the sections were blocked with 5% normal goat serum for 30 min and sequentially incubated with anti–*C. albicans* (Thermo Fisher Scientific) antibody and fluorophore-tagged secondary antibodies. Samples were counterstained with fluorescein isothiocyanate (FITC)–conjugated UEA-1 (for mucin) for 45 min at 4°C. Last, sections were mounted with ProLong Diamond (Thermo Fisher Scientific) and imaged with Zeiss LSM710.

Single-cell RNA sequencing

Femur BM cells were harvested from four PBS-treated and four *C. albicans*–colonized female mice. Cells from individual mouse were hashtagged using the 3′ CellPlex Kit Set A (10x Genomics PN-1000261) according to the manufacturer′s protocol and counted using a Bio-Rad TC20 automated cell counter. Single cells were then encapsulated into emulsion droplets using Chromium Controller (10x Genomics). scRNA-seq and cell multiplexing libraries were constructed using Chromium Single Cell 3′ version 3.1 Reagent Kit and 3′ Feature Barcode Kit (PN-1000268 and 1000262, respectively) according to the manufacturer′s protocol. Amplified complementary DNA was evaluated on an Agilent BioAnalyzer 2100 using a High-Sensitivity DNA Kit (Agilent Technologies) and final libraries on an Agilent TapeStation 4200 using High-Sensitivity D1000 ScreenTape (Agilent Technologies). Individual libraries were diluted to 2 nM and pooled for sequencing. Pools were sequenced with 100-cycle run kits (28-bp Read1, 8-bp

Index1, and 91-bp Read2) on the NovaSeq 6000 Sequencing System (Illumina).

scRNA-seq data processing

The CellRanger′s pipeline version 7.0.0 was used to demultiplex cellular barcodes and aligned reads against the mouse genome (mm10 ensemble). Downstream RNA-seq analysis was done with Seurat version 4.0.0 on R version 4.2.1 with the filtered RNA and lipid-derived hashtag oligo (HTO) featured counts. Cells containing more than 20% mitochondrial DNA and less than 300 feature genes were filtered out for initial quality control. HTOs were normalized using centered log ratio transformation and demultiplexed with the function HTODemux to identify doublets; additional doublets were removed using the scDblFinder package with a calculated doublet rate of 0.14. Regularized negative binomial regression was performed for RNA normalization using the SCTranformation function. Principle components analysis was performed, and the Louvain algorithm determined unsupervised clustering with 20 dimensions. Uniform manifold approximation and projection representation based on totalVI dimension reduction of RNA was used to visualize data. Cell types were determined by a combination of unbiases clustering, canonical cell type marker signatures, and cell type annotation via the SingleR package with the ImmGenData and MouseRNAseqData open-source (expression) reference databases in the CellDex package. The Wilcox test assessed differentially expressed genes between clusters and treatment groups with a Benjamin-Hochberg *P* value adjustment.

Bacteria strains and growth conditions

S. aureus strain USA300 LAC clone AH1263 (*96*), *S. pneumoniae* P2406 (serotype 4, strain TIGR4; clinical isolate with streptomycin resistance) (*97*), and *S. pneumoniae* P2090 (serotype 3; ATCC 6303) were used for in vivo infection studies. *S. aureus* strains were grown on TSA or TSB. *S. aureus* cultures were grown in 5 ml of medium in 15-ml tubes shaking with a 45° angle at 37°C. For all experiments, *S. aureus* was grown in TSB overnight and a 1:100 dilution of overnight cultures was subcultured into fresh TSB. *S. aureus* grown to early stationary phase (3 h) was collected and normalized by optical density at 600 nm for further experimental analysis. *S. pneumoniae* P2406 and P2090 were grown statically in TSB at 37°C to mid-log phase (optical density of 1.0 at 620 nm), washed once in Dulbecco′s PBS (dPBS), and diluted to obtain a dose of 100 CFU/gram of body weight in 100 μl of dPBS and a dose of 10^4 CFU in 80 μl of dPBS respectively.

In vivo infections

Mice under antibiotics treatment were inoculated with wild-type *C. albicans* or mutant strains and colonized for 21 days. Twenty-four hours before bacterial challenge, antibiotics in drinking water was replaced to regular water. For *S. aureus* infection, mice were anesthetized with Avertin [2,2,2-tribromoethanol dissolved in tert-amyl alcohol and diluted to a final concentration of 2.5% (v/v) in 0.9% sterile saline] by intraperitoneal injection. Mice then were challenged with 1×10^7 CFUs by retro-orbital injection. Signs of morbidity (>30% weight loss, ruffled fur, hunched posture, paralysis, inability to walk, or inability to consume food or water) were monitored after infection. For *S. pneumoniae* P2406 infection, mice were inoculated via the intraperitoneal route and monitored daily after infection. For intranasal inoculation, mice were administered *S. pneumoniae* P2090 after anesthesia with isoflurane and monitored daily.

Quantification and statistical analysis

Statistical parameters including the definition of central value and the exact number (*n*) of mice per group are annotated in the corresponding figure legend. Results in graphs and bar plots are displayed as mean ± SD. Statistical analysis was performed with GraphPad Prism version 9.2 for Mac (GraphPad) by using an unpaired two-tailed Student′s t test to evaluate differences between two groups. For statistical analysis of multiple groups, the ordinary one-way analysis of variance (ANOVA) with Holm-Šidák multiple comparisons test was applied. For statistical analysis of survival among groups, log-rank Mantel-Cox test was applied. (∗*P* value < 0.05, ∗∗*P* value < 0.01, ∗∗∗*P* value < 0.001, and ∗∗∗∗*P* value < 0.0001; ns, not statistically significant).

Supplementary Materials

This PDF file includes:
Figs. S1 to S6
Table S1 to S3
Reference (*98*)

Other Supplementary Material for this manuscript includes the following:
Data file S1
MDAR Reproducibility Checklist

View/request a protocol for this paper from *Bio-protocol*.

REFERENCES AND NOTES

1. S. Rakoff-Nahoum, J. Paglino, F. Eslami-Varzaneh, S. Edberg, R. Medzhitov, Recognition of commensal microflora by Toll-like receptors is required for intestinal homeostasis. *Cell* **118**, 229–241 (2004).
2. K. Smith, K. D. McCoy, A. J. Macpherson, Use of axenic animals in studying the adaptation of mammals to their commensal intestinal microbiota. *Semin. Immunol.* **19**, 59–69 (2007).
3. I. I. Ivanov, K. Atarashi, N. Manel, E. L. Brodie, T. Shima, U. Karaoz, D. Wei, K. C. Goldfarb, C. A. Santee, S. V. Lynch, T. Tanoue, A. Imaoka, K. Itoh, K. Takeda, Y. Umesaki, K. Honda, D. R. Littman, Induction of intestinal Th17 cells by segmented filamentous bacteria. *Cell* **139**, 485–498 (2009).
4. D. A. Hill, C. Hoffmann, M. C. Abt, Y. du, D. Kobuley, T. J. Kirn, F. D. Bushman, D. Artis, Metagenomic analyses reveal antibiotic-induced temporal and spatial changes in intestinal microbiota with associated alterations in immune cell homeostasis. *Mucosal Immunol.* **3**, 148–158 (2010).
5. D. S. Lima-Junior, S. R. Krishnamurthy, N. Bouladoux, N. Collins, S. J. Han, E. Y. Chen, M. G. Constantinides, V. M. Link, A. I. Lim, M. Enamorado, C. Cataisson, L. Gil, I. Rao, T. K. Farley, G. Koroleva, J. Attig, S. H. Yuspa, M. A. Fischbach, G. Kassiotis, Y. Belkaid, Endogenous retroviruses promote homeostatic and inflammatory responses to the microbiota. *Cell* **184**, 3794–3811.e19 (2021).
6. J. Mestas, C. C. W. Hughes, Of mice and not men: Differences between mouse and human immunology. *J. Immunol.* **172**, 2731–2738 (2004).
7. L. Tao, T. A. Reese, Making mouse models that reflect human immune responses. *Trends Immunol.* **38**, 181–193 (2017).
8. D. Masopust, C. P. Sivula, S. C. Jameson, Of mice, dirty mice, and men: Using mice to understand human immunology. *J. Immunol.* **199**, 383–388 (2017).
9. L. K. Beura, S. E. Hamilton, K. Bi, J. M. Schenkel, O. A. Odumade, K. A. Casey, E. A. Thompson, K. A. Fraser, P. C. Rosato, A. Filali-Mouhim, R. P. Sekaly, M. K. Jenkins, V. Vezys, W. N. Haining, S. C. Jameson, D. Masopust, Normalizing the environment recapitulates adult human immune traits in laboratory mice. *Nature* **532**, 512–516 (2016).
10. T. A. Reese, K. Bi, A. Kambal, A. Filali-Mouhim, L. K. Beura, M. C. Bürger, B. Pulendran, R. P. Sekaly, S. C. Jameson, D. Masopust, W. N. Haining, H. W. Virgin, Sequential infection with common pathogens promotes human-like immune gene expression and altered vaccine response. *Cell Host Microbe* **19**, 713–719 (2016).

11. Y. J. Choi, S. Kim, Y. Choi, T. B. Nielsen, J. Yan, A. Lu, J. Ruan, H. R. Lee, H. Wu, B. Spellberg, J. U. Jung, SERPINB1-mediated checkpoint of inflammatory caspase activation. *Nat. Immunol.* **20**, 276–287 (2019).
12. J. K. Fiege, K. E. Block, M. J. Pierson, H. Nanda, F. K. Shepherd, C. K. Mickelson, J. M. Stolley, W. E. Matchett, S. Wijeyesinghe, D. K. Meyerholz, V. Vezys, S. S. Shen, S. E. Hamilton, D. Masopust, R. A. Langlois, Mice with diverse microbial exposure histories as a model for preclinical vaccine testing. *Cell Host Microbe* **29**, 1815–1827.e6 (2021).
13. S. P. Rosshart, J. Herz, B. G. Vassallo, A. Hunter, M. K. Wall, J. H. Badger, J. A. McCulloch, D. G. Anastasakis, A. A. Sarshad, I. Leonardi, N. Collins, J. A. Blatter, S. J. Han, S. Tamoutounour, S. Potapova, M. B. Foster St. Claire, W. Yuan, S. K. Sen, M. S. Dreier, B. Hild, M. Hafner, D. Wang, I. D. Iliev, Y. Belkaid, G. Trinchieri, B. Rehermann, Laboratory mice born to wild mice have natural microbiota and model human immune responses. *Science* **365**, eaaw4361 (2019).
14. S. P. Rosshart, B. G. Vassallo, D. Angeletti, D. S. Hutchinson, A. P. Morgan, K. Takeda, H. D. Hickman, J. A. McCulloch, J. H. Badger, N. J. Ajami, G. Trinchieri, F. Pardo-Manuel de Villena, J. W. Yewdell, B. Rehermann, Wild mouse gut microbiota promotes host fitness and improves disease resistance. *Cell* **171**, 1015–1028.e13 (2017).
15. J. M. Leung, S. A. Budischak, H. Chung The, C. Hansen, R. Bowcutt, R. Neill, M. Shellman, P. Loke, A. L. Graham, Rapid environmental effects on gut nematode susceptibility in rewilded mice. *PLoS Biol.* **16**, e2004108 (2018).
16. F. Yeung, Y. H. Chen, J. D. Lin, J. M. Leung, C. McCauley, J. C. Devlin, C. Hansen, A. Cronkite, Z. Stephens, C. Drake-Dunn, Y. Fulmer, B. Shopsin, K. V. Ruggles, J. L. Round, P. Loke, A. L. Graham, K. Cadwell, Altered immunity of laboratory mice in the natural environment is associated with fungal colonization. *Cell Host Microbe* **27**, 809–822.e6 (2020).
17. J. D. Lin, J. C. Devlin, F. Yeung, C. McCauley, J. M. Leung, Y. H. Chen, A. Cronkite, C. Hansen, C. Drake-Dunn, K. V. Ruggles, K. Cadwell, A. L. Graham, P. Loke, Rewilding Nod2 and Atg16l1 mutant mice uncovers genetic and environmental contributions to microbial responses and immune cell composition. *Cell Host Microbe* **27**, 830–840.e4 (2020).
18. F. C. Odds, A. D. Davidson, M. D. Jacobsen, A. Tavanti, J. A. Whyte, C. C. Kibbler, D. H. Ellis, M. C. J. Maiden, D. J. Shaw, N. A. R. Gow, *Candida albicans* strain maintenance, replacement, and microvariation demonstrated by multilocus sequence typing. *J. Clin. Microbiol.* **44**, 3647–3658 (2006).
19. J. Kim, P. Sudbery, *Candida albicans*, a major human fungal pathogen. *J. Microbiol.* **49**, 171–177 (2011).
20. C. Rao, K. Z. Coyte, W. Bainter, R. S. Geha, C. R. Martin, S. Rakoff-Nahoum, Multi-kingdom ecological drivers of microbiota assembly in preterm infants. *Nature* **591**, 633–638 (2021).
21. F. L. Mayer, D. Wilson, B. Hube, *Candida albicans* pathogenicity mechanisms. *Virulence* **4**, 119–128 (2013).
22. D. S. Thompson, P. L. Carlisle, D. Kadosh, Coevolution of morphology and virulence in Candida species. *Eukaryot. Cell* **10**, 1173–1182 (2011).
23. J. N. Witchley, P. Penumetcha, N. V. Abon, C. A. Woolford, A. P. Mitchell, S. M. Noble, *Candida albicans* morphogenesis programs control the balance between gut commensalism and invasive infection. *Cell Host Microbe* **25**, 432–443.e6 (2019).
24. I. Doron, M. Mesko, X. V. Li, T. Kusakabe, I. Leonardi, D. G. Shaw, W. D. Fiers, W. Y. Lin, M. Bialt-DeCelie, E. Román, R. S. Longman, J. Pla, P. C. Wilson, I. D. Iliev, Mycobiota-induced IgA antibodies regulate fungal commensalism in the gut and are dysregulated in Crohn's disease. *Nat. Microbiol.* **6**, 1493–1504 (2021).
25. S. H. Liang, M. Z. Anderson, M. P. Hirakawa, J. M. Wang, C. Frazer, L. M. Alaalm, G. J. Thomson, I. V. Ene, R. J. Bennett, Hemizygosity enables a mutational transition governing fungal virulence and commensalism. *Cell Host Microbe* **25**, 418–431.e6 (2019).
26. K. S. Ost, T. R. O'Meara, W. Z. Stephens, T. Chiaro, H. Zhou, J. Penman, R. Bell, J. R. Catanzaro, D. Song, S. Singh, D. H. Call, E. Hwang-Wong, K. E. Hanson, J. F. Valentine, K. A. Christensen, R. M. O'Connell, B. Cormack, A. S. Ibrahim, N. W. Palm, S. M. Noble, J. L. Round, Adaptive immunity induces mutualism between commensal eukaryotes. *Nature* **596**, 114–118 (2021).
27. G. H. W. Tso, J. A. Reales-Calderon, A. S. M. Tan, X. H. Sem, G. T. T. le, T. G. Tan, G. C. Lai, K. G. Srinivasan, M. Yurieva, W. Liao, M. Poidinger, F. Zolezzi, G. Rancati, N. Pavelka, Experimental evolution of a fungal pathogen into a gut symbiont. *Science* **362**, 589–595 (2018).
28. P. Bacher, T. Hohnstein, E. Beerbaum, M. Röcker, M. G. Blango, S. Kaufmann, J. Röhmel, P. Eschenhagen, C. Grehn, K. Seidel, V. Rickerts, L. Lozza, U. Stervbo, M. Nienen, N. Babel, J. Milleck, M. Assenmacher, O. A. Cornely, M. Ziegler, H. Wisplinghoff, G. Heine, M. Worm, B. Siegmund, J. Maul, P. Creutz, C. Tabeling, C. Ruwwe-Glösenkamp, L. E. Sander, C. Knosalla, S. Brunke, B. Hube, O. Kniemeyer, A. A. Brakhage, C. Schwarz, A. Scheffold, Human anti-fungal Th17 immunity and pathology rely on cross-reactivity against *Candida albicans*. *Cell* **176**, 1340–1355.e15 (2019).
29. T. T. Jiang, T. Y. Shao, W. X. G. Ang, J. M. Kinder, L. H. Turner, G. Pham, J. Whitt, T. Alenghat, S. S. Way, Commensal fungi recapitulate the protective benefits of intestinal bacteria. *Cell Host Microbe* **22**, 809–816.e4 (2017).
30. T. Y. Shao, W. X. G. Ang, T. T. Jiang, F. S. Huang, H. Andersen, J. M. Kinder, G. Pham, A. R. Burg, B. Ruff, T. Gonzalez, G. K. Khurana Hershey, D. B. Haslam, S. S. Way, Commensal *Candida albicans* positively calibrates systemic Th17 immunological responses. *Cell Host Microbe* **25**, 404–417.e6 (2019).
31. I. Leonardi, I. H. Gao, W. Y. Lin, M. Allen, X. V. Li, W. D. Fiers, M. B. de Celie, G. G. Putzel, R. K. Yantiss, M. Johncilla, D. Colak, I. D. Iliev, Mucosal fungi promote gut barrier function and social behavior via type 17 immunity. *Cell* **185**, 831–846.e14 (2022).
32. K. Atarashi, T. Tanoue, M. Ando, N. Kamada, Y. Nagano, S. Narushima, W. Suda, A. Imaoka, H. Setoyama, T. Nagamori, E. Ishikawa, T. Shima, T. Hara, S. Kado, T. Jinnohara, H. Ohno, T. Kondo, K. Toyooka, E. Watanabe, S. I. Yokoyama, S. Tokoro, H. Mori, Y. Noguchi, H. Morita, I. I. Ivanov, T. Sugiyama, G. Nuñez, J. G. Camp, M. Hattori, Y. Umesaki, K. Honda, Th17 cell induction by adhesion of microbes to intestinal epithelial cells. *Cell* **163**, 367–380 (2015).
33. H. R. Conti, F. Shen, N. Nayyar, E. Stocum, J. N. Sun, M. J. Lindemann, A. W. Ho, J. H. Hai, J. J. Yu, J. W. Jung, S. G. Filler, P. Masso-Welch, M. Edgerton, S. L. Gaffen, Th17 cells and IL-17 receptor signaling are essential for mucosal host defense against oral candidiasis. *J. Exp. Med.* **206**, 299–311 (2009).
34. H. Hirai, P. Zhang, T. Dayaram, C. J. Hetherington, S. I. Mizuno, J. Imanishi, K. Akashi, D. G. Tenen, C/EBPbeta is required for 'emergency' granulopoiesis. *Nat. Immunol.* **7**, 732–739 (2006).
35. I. Mitroulis, L. Kalafati, G. Hajishengallis, T. Chavakis, Myelopoiesis in the context of innate immunity. *J. Innate Immun.* **10**, 365–372 (2018).
36. M. G. Manz, S. Boettcher, Emergency granulopoiesis. *Nat. Rev. Immunol.* **14**, 302–314 (2014).
37. S. Bekkering, R. J. W. Arts, B. Novakovic, I. Kourtzelis, C. D. C. C. van der Heijden, Y. Li, C. D. Popa, R. ter Horst, J. van Tuijl, R. T. Netea-Maier, F. L. van de Veerdonk, T. Chavakis, L. A. B. Joosten, J. W. M. van der Meer, H. Stunnenberg, N. P. Riksen, M. G. Netea, Metabolic induction of trained immunity through the mevalonate pathway. *Cell* **172**, 135–146.e9 (2018).
38. J. C. D. Santos, A. M. B. de Figueiredo, M. V. T. Silva, B. Cirovic, L. C. J. de Bree, M. S. M. A. Damen, S. J. C. F. M. Moorlag, R. S. Gomes, M. M. Helsen, M. Oosting, S. T. Keating, A. Schlitzer, M. G. Netea, F. Ribeiro-Dias, L. A. B. Joosten, β-Glucan-induced trained immunity protects against *Leishmania braziliensis* infection: A crucial role for IL-32. *Cell Rep.* **28**, 2659–2672.e6 (2019).
39. S. J. C. F. M. Moorlag, N. Khan, B. Novakovic, E. Kaufmann, T. Jansen, R. van Crevel, M. Divangahi, M. G. Netea, β-Glucan induces protective trained immunity against mycobacterium tuberculosis infection: A key role for IL-1. *Cell Rep.* **31**, 107634 (2020).
40. M. G. Netea, L. A. B. Joosten, E. Latz, K. H. G. Mills, G. Natoli, H. G. Stunnenberg, L. A. J. O'Neill, R. J. Xavier, Trained immunity: A program of innate immune memory in health and disease. *Science* **352**, aaf1098 (2016).
41. J. Quintin, S. Saeed, J. H. A. Martens, E. J. Giamarellos-Bourboulis, D. C. Ifrim, C. Logie, L. Jacobs, T. Jansen, B. J. Kullberg, C. Wijmenga, L. A. B. Joosten, R. J. Xavier, J. W. M. van der Meer, H. G. Stunnenberg, M. G. Netea, *Candida albicans* infection affords protection against reinfection via functional reprogramming of monocytes. *Cell Host Microbe* **12**, 223–232 (2012).
42. S. C. Cheng, J. Quintin, R. A. Cramer, K. M. Shepardson, S. Saeed, V. Kumar, E. J. Giamarellos-Bourboulis, J. H. A. Martens, N. A. Rao, A. Aghajanirefah, G. R. Manjeri, Y. Li, D. C. Ifrim, R. J. W. Arts, B. M. J. W. van der Veer, P. M. T. Deen, C. Logie, L. A. O'Neill, P. Willems, F. L. van de Veerdonk, J. W. M. van der Meer, A. Ng, L. A. B. Joosten, C. Wijmenga, H. G. Stunnenberg, R. J. Xavier, M. G. Netea, mTOR- and HIF-1α–mediated aerobic glycolysis as metabolic basis for trained immunity. *Science* **345**, 1250684 (2014).
43. P. R. Taylor, G. D. Brown, D. M. Reid, J. A. Willment, L. Martinez-Pomares, S. Gordon, S. Y. C. Wong, The beta-glucan receptor, dectin-1, is predominantly expressed on the surface of cells of the monocyte/macrophage and neutrophil lineages. *J. Immunol.* **169**, 3876–3882 (2002).
44. S. Walachowski, G. Tabouret, M. Fabre, G. Foucras, Molecular analysis of a short-term model of β-glucans-trained immunity highlights the accessory contribution of GM-CSF in priming mouse macrophages response. *Front. Immunol.* **8**, 1089 (2017).
45. I. Leonardi, X. Li, A. Semon, D. Li, I. Doron, G. Putzel, A. Bar, D. Prieto, M. Rescigno, D. P. B. McGovern, J. Pla, I. D. Iliev, CX3CR1^{+} mononuclear phagocytes control immunity to intestinal fungi. *Science* **359**, 232–236 (2018).
46. J. M. Adrover, C. del Fresno, G. Crainiciuc, M. I. Cuartero, M. Casanova-Acebes, L. A. Weiss, H. Huerga-Encabo, C. Silvestre-Roig, J. Rossaint, I. Cossío, A. V. Lechuga-Vieco, J. García-Prieto, M. Gómez-Parrizas, J. A. Quintana, I. Ballesteros, S. Martin-Salamanca, A. Aroca-Crevillen, S. Z. Chong, M. Evrard, K. Balabanian, J. López, K. Bidzhekov, F. Bachelerie, F. Abad-Santos, C. Muñoz-Calleja, A. Zarbock, O. Soehnlein, C. Weber, L. G. Ng, C. Lopez-Rodriguez, D. Sancho, M. A. Moro, B. Ibáñez, A. Hidalgo, A neutrophil timer coordinates immune defense and vascular protection. *Immunity* **50**, 390–402.e10 (2019).
47. M. Casanova-Acebes, C. Pitaval, L. A. Weiss, C. Nombela-Arrieta, R. Chèvre, N. A-González, Y. Kunisaki, D. Zhang, N. van Rooijen, L. E. Silberstein, C. Weber, T. Nagasawa, P. S. Frenette,

A. Castrillo, A. Hidalgo, Rhythmic modulation of the hematopoietic niche through neutrophil clearance. *Cell* **153**, 1025–1035 (2013).
48. E. M. Pietras, D. Reynaud, Y. A. Kang, D. Carlin, F. J. Calero-Nieto, A. D. Leavitt, J. M. Stuart, B. Göttgens, E. Passegué, Functionally distinct subsets of lineage-biased multipotent progenitors control blood production in normal and regenerative conditions. *Cell Stem Cell* **17**, 35–46 (2015).
49. A. Wilson, E. Laurenti, G. Oser, R. C. van der Wath, W. Blanco-Bose, M. Jaworski, S. Offner, C. F. Dunant, L. Eshkind, E. Bockamp, P. Lió, H. R. MacDonald, A. Trumpp, Hematopoietic stem cells reversibly switch from dormancy to self-renewal during homeostasis and repair. *Cell* **135**, 1118–1129 (2008).
50. M. Evrard, I. W. H. Kwok, S. Z. Chong, K. W. W. Teng, E. Becht, J. Chen, J. L. Sieow, H. L. Penny, G. C. Ching, S. Devi, J. M. Adrover, J. L. Y. Li, K. H. Liong, L. Tan, Z. Poon, S. Foo, J. W. Chua, I. H. Su, K. Balabanian, F. Bachelerie, S. K. Biswas, A. Larbi, W. Y. K. Hwang, V. Madan, H. P. Koeffler, S. C. Wong, E. W. Newell, A. Hidalgo, F. Ginhoux, L. G. Ng, Developmental analysis of bone marrow neutrophils reveals populations specialized in expansion, trafficking, and effector functions. *Immunity* **48**, 364–379.e8 (2018).
51. H. S. Goodridge, A. J. Wolf, D. M. Underhill, Beta-glucan recognition by the innate immune system. *Immunol. Rev.* **230**, 38–50 (2009).
52. E. S. Theel, C. D. Doern, Point-counterpoint: β-d-Glucan testing is important for diagnosis of invasive fungal infections. *J. Clin. Microbiol.* **51**, 3478–3483 (2013).
53. A. Carvalho, G. Giovannini, A. de Luca, C. D'Angelo, A. Casagrande, R. G. Iannitti, G. Ricci, C. Cunha, L. Romani, Dectin-1 isoforms contribute to distinct Th1/Th17 cell activation in mucosal candidiasis. *Cell. Mol. Immunol.* **9**, 276–286 (2012).
54. K. L. Flannigan, V. L. Ngo, D. Geem, A. Harusato, S. A. Hirota, C. A. Parkos, N. W. Lukacs, A. Nusrat, V. Gaboriau-Routhiau, N. Cerf-Bensussan, A. T. Gewirtz, T. L. Denning, IL-17A-mediated neutrophil recruitment limits expansion of segmented filamentous bacteria. *Mucosal Immunol.* **10**, 673–684 (2017).
55. T. Jouault, S. Ibata-Ombetta, O. Takeuchi, P.-A. Trinel, P. Sacchetti, P. Lefebvre, S. Akira, D. Poulain, *Candida albicans* phospholipomannan is sensed through toll-like receptors. *J. Infect. Dis.* **188**, 165–172 (2003).
56. K. Fuchs, Y. Cardona Gloria, O. O. Wolz, F. Herster, L. Sharma, C. A. Dillen, C. Täumer, S. Dickhöfer, Z. Bittner, T. M. Dang, A. Singh, D. Haischer, M. A. Schlöffel, K. J. Koymans, T. Sanmuganantham, M. Krach, T. Roger, D. le Roy, N. A. Schilling, F. Frauhammer, L. S. Miller, T. Nürnberger, S. LeibundGut-Landmann, A. A. Gust, B. Macek, M. Frank, C. Gouttefangeas, C. S. dela Cruz, D. Hartl, A. N. R. Weber, The fungal ligand chitin directly binds TLR2 and triggers inflammation dependent on oligomer size. *EMBO Rep.* **19**, a46065 (2018).
57. J. Wagener, R. K. S. Malireddi, M. D. Lenardon, M. Köberle, S. Vautier, D. M. MacCallum, T. Biedermann, M. Schaller, M. G. Netea, T. D. Kanneganti, G. D. Brown, A. J. P. Brown, N. A. R. Gow, Fungal chitin dampens inflammation through IL-10 induction mediated by NOD2 and TLR9 activation. *PLOS Pathog.* **10**, e1004050 (2014).
58. P. Schwarzenberger, V. la Russa, A. Miller, P. Ye, W. Huang, A. Zieske, S. Nelson, G. J. Bagby, D. Stoltz, R. L. Mynatt, M. Spriggs, J. K. Kolls, IL-17 stimulates granulopoiesis in mice: Use of an alternate, novel gene therapy-derived method for in vivo evaluation of cytokines. *J. Immunol.* **161**, 6383–6389 (1998).
59. M. A. Stark, Y. Huo, T. L. Burcin, M. A. Morris, T. S. Olson, K. Ley, Phagocytosis of apoptotic neutrophils regulates granulopoiesis via IL-23 and IL-17. *Immunity* **22**, 285–294 (2005).
60. D. Metcalf, Hematopoietic cytokines. *Blood* **111**, 485–491 (2008).
61. A. C. Berardi, A. Wang, J. D. Levine, P. Lopez, D. T. Scadden, Functional isolation and characterization of human hematopoietic stem cells. *Science* **267**, 104–108 (1995).
62. K. Maeda, A. Malykhin, B. N. Teague-Weber, X. H. Sun, A. D. Farris, K. M. Coggeshall, Interleukin-6 aborts lymphopoiesis and elevates production of myeloid cells in systemic lupus erythematosus-prone B6.Sle1.Yaa animals. *Blood* **113**, 4534–4540 (2009).
63. L. Mukaremera, K. K. Lee, H. M. Mora-Montes, N. A. R. Gow, *Candida albicans* yeast, pseudohyphal, and hyphal morphogenesis differentially affects immune recognition. *Front. Immunol.* **8**, 629 (2017).
64. B. N. Gantner, R. M. Simmons, D. M. Underhill, Dectin-1 mediates macrophage recognition of *Candida albicans* yeast but not filaments. *EMBO J.* **24**, 1277–1286 (2005).
65. C. d'Enfert, A. K. Kaune, L. R. Alaban, S. Chakraborty, N. Cole, M. Delavy, D. Kosmala, B. Marsaux, R. Fróis-Martins, M. Morelli, D. Rosati, M. Valentine, Z. Xie, Y. Emritloll, P. A. Warn, F. Bequet, M. E. Bougnoux, S. Bornes, M. S. Gresnigt, B. Hube, I. D. Jacobsen, M. Legrand, S. Leibundgut-Landmann, C. Manichanh, C. A. Munro, M. G. Netea, K. Queiroz, K. Roget, V. Thomas, C. Thoral, P. van den Abbeele, A. W. Walker, A. J. P. Brown, The impact of the fungus-host-microbiota interplay upon *Candida albicans* infections: Current knowledge and new perspectives. *FEMS Microbiol. Rev.* **45**, fuaa060 (2021).
66. F. Cao, S. Lane, P. P. Raniga, Y. Lu, Z. Zhou, K. Ramon, J. Chen, H. Liu, The Flo8 transcription factor is essential for hyphal development and virulence in *Candida albicans*. *Mol. Biol. Cell* **17**, 295–307 (2006).
67. K. Sohn, C. Urban, H. Brunner, S. Rupp, EFG1 is a major regulator of cell wall dynamics in *Candida albicans* as revealed by DNA microarrays. *Mol. Microbiol.* **47**, 89–102 (2003).
68. S. Lane, C. Birse, S. Zhou, R. Matson, H. Liu, DNA array studies demonstrate convergent regulation of virulence factors by Cph1, Cph2, and Efg1 in *Candida albicans*. *J. Biol. Chem.* **276**, 48988–48996 (2001).
69. J. M. Hollomon, Z. Liu, S. F. Rusin, N. P. Jenkins, A. K. Smith, K. Koeppen, A. N. Kettenbach, L. C. Myers, D. A. Hogan, The *Candida albicans* Cdk8-dependent phosphoproteome reveals repression of hyphal growth through a Flo8-dependent pathway. *PLOS Genet.* **18**, e1009622 (2022).
70. D. L. Moyes, D. Wilson, J. P. Richardson, S. Mogavero, S. X. Tang, J. Wernecke, S. Höfs, R. L. Gratacap, J. Robbins, M. Runglall, C. Murciano, M. Blagojevic, S. Thavaraj, T. M. Förster, B. Hebecker, L. Kasper, G. Vizcay, S. I. Iancu, N. Kichik, A. Häder, O. Kurzai, T. Luo, T. Krüger, O. Kniemeyer, E. Cota, O. Bader, R. T. Wheeler, T. Gutsmann, B. Hube, J. R. Naglik, Candidalysin is a fungal peptide toxin critical for mucosal infection. *Nature* **532**, 64–68 (2016).
71. K. M. Rigby, F. R. DeLeo, Neutrophils in innate host defense against *Staphylococcus aureus* infections. *Semin. Immunopathol.* **34**, 237–259 (2012).
72. I. Doron, I. Leonardi, X. V. Li, W. D. Fiers, A. Semon, M. Bialt-DeCelie, M. Migaud, I. H. Gao, W. Y. Lin, T. Kusakabe, A. Puel, I. D. Iliev, Human gut mycobiota tune immunity via CARD9-dependent induction of anti-fungal IgG antibodies. *Cell* **184**, 1017–1031.e14 (2021).
73. R. Arrazuria, B. Kerscher, K. E. Huber, J. L. Hoover, C. V. Lundberg, J. U. Hansen, S. Sordello, S. Renard, V. Aranzana-Climent, D. Hughes, P. Gribbon, L. E. Friberg, I. Bekeredjian-Ding, Variability of murine bacterial pneumonia models used to evaluate antimicrobial agents. *Front. Microbiol.* **13**, 988728 (2022).
74. S. Fanucchi, J. Dominguez-Andres, L. A. B. Joosten, M. G. Netea, M. M. Mhlanga, The intersection of epigenetics and metabolism in trained immunity. *Immunity* **54**, 32–43 (2021).
75. E. Ciarlo, T. Heinonen, C. Théroude, F. Asgari, D. le Roy, M. G. Netea, T. Roger, Trained immunity confers broad-spectrum protection against bacterial infections. *J Infect Dis* **222**, 1869–1881 (2020).
76. I. Mitroulis, K. Ruppova, B. Wang, L. S. Chen, M. Grzybek, T. Grinenko, A. Eugster, M. Troullinaki, A. Palladini, I. Kourtzelis, A. Chatzigeorgiou, A. Schlitzer, M. Beyer, L. A. B. Joosten, B. Isermann, M. Lesche, A. Petzold, K. Simons, I. Henry, A. Dahl, J. L. Schultze, B. Wielockx, N. Zamboni, P. Mirtschink, Ü. Coskun, G. Hajishengallis, M. G. Netea, T. Chavakis, Modulation of myelopoiesis progenitors is an integral component of trained immunity. *Cell* **172**, 147–161.e12 (2018).
77. T. S. Mims, Q. A. Abdallah, J. D. Stewart, S. P. Watts, C. T. White, T. V. Rousselle, A. Gosain, A. Bajwa, J. C. Han, K. A. Willis, J. F. Pierre, The gut mycobiome of healthy mice is shaped by the environment and correlates with metabolic outcomes in response to diet. *Commun. Biol.* **4**, 281 (2021).
78. X. V. Li, I. Leonardi, G. G. Putzel, A. Semon, W. D. Fiers, T. Kusakabe, W. Y. Lin, I. H. Gao, I. Doron, A. Gutierrez-Guerrero, M. B. DeCelie, G. M. Carriche, M. Mesko, C. Yang, J. R. Naglik, B. Hube, E. J. Scherl, I. D. Iliev, Immune regulation by fungal strain diversity in inflammatory bowel disease. *Nature* **603**, 672–678 (2022).
79. I. D. Iliev, K. Cadwell, Effects of intestinal fungi and viruses on immune responses and inflammatory bowel diseases. *Gastroenterology* **160**, 1050–1066 (2021).
80. A. L. Graham, Naturalizing mouse models for immunology. *Nat. Immunol.* **22**, 111–117 (2021).
81. J. A. Reales-Calderon, G. H. W. Tso, A. S. M. Tan, P. X. Hor, J. Böhme, K. W. W. Teng, E. W. Newell, A. Singhal, N. Pavelka, Gut-evolved *Candida albicans* induces metabolic changes in neutrophils. *Front. Cell. Infect. Microbiol.* **11**, 743735 (2021).
82. T. Y. Shao, P. Kakade, J. N. Witchley, C. Frazer, K. L. Murray, I. V. Ene, D. B. Haslam, T. Hagan, S. M. Noble, R. J. Bennett, S. S. Way, *Candida albicans* oscillating UME6 expression during intestinal colonization primes systemic Th17 protective immunity. *Cell Rep.* **39**, 110837 (2022).
83. F. Borriello, V. Poli, E. Shrock, R. Spreafico, X. Liu, N. Pishesha, C. Carpenet, J. Chou, M. di Gioia, M. E. McGrath, C. A. Dillen, N. A. Barrett, L. Lacanfora, M. E. Franco, L. Marongiu, Y. Iwakura, F. Pucci, M. D. Kruppa, Z. Ma, D. W. Lowman, H. E. Ensley, E. Nanishi, Y. Saito, T. R. O'Meara, H. S. Seo, S. Dhe-Paganon, D. J. Dowling, M. Frieman, S. J. Elledge, O. Levy, D. J. Irvine, H. L. Ploegh, D. L. Williams, I. Zanoni, An adjuvant strategy enabled by modulation of the physical properties of microbial ligands expands antigen immunogenicity. *Cell* **185**, 614–629.e21 (2022).
84. B. M. Peters, E. S. Ovchinnikova, B. P. Krom, L. M. Schlecht, H. Zhou, L. L. Hoyer, H. J. Busscher, H. C. van der Mei, M. A. Jabra-Rizk, M. E. Shirtliff, *Staphylococcus aureus* adherence to *Candida albicans* hyphae is mediated by the hyphal adhesin Als3p. *Microbiology (Reading)* **158**, 2975–2986 (2012).
85. K. Van Dyck, F. Viela, M. Mathelié-Guinlet, L. Demuyser, E. Hauben, M. A. Jabra-Rizk, G. V. Velde, Y. F. Dufrêne, B. P. Krom, P. Van Dijck, Adhesion of *Staphylococcus aureus* to *Candida albicans* during co-infection promotes bacterial dissemination through the host immune response. *Front. Cell. Infect. Microbiol.* **10**, 624839 (2020).
86. O. A. Todd, P. L. Fidel Jr., J. M. Harro, J. J. Hilliard, C. Tkaczyk, B. R. Sellman, M. C. Noverr, B. M. Peters, *Candida albicans* augments *Staphylococcus aureus* virulence by engaging the staphylococcal agr quorum sensing system. *MBio* **10**, e00910-19 (2019).

87. S. Basu, G. Hodgson, H. H. Zhang, M. Katz, C. Quilici, A. R. Dunn, "Emergency" granulopoiesis in G-CSF-deficient mice in response to *Candida albicans* infection. *Blood* **95**, 3725–3733 (2000).
88. C. Silvestre-Roig, Q. Braster, A. Ortega-Gomez, O. Soehnlein, Neutrophils as regulators of cardiovascular inflammation. *Nat. Rev. Cardiol.* **17**, 327–340 (2020).
89. E. B. Eruslanov, S. Singhal, S. M. Albelda, Mouse versus human neutrophils in cancer: A major knowledge gap. *Trends Cancer* **3**, 149–160 (2017).
90. C. C. Hedrick, I. Malanchi, Neutrophils in cancer: Heterogeneous and multifaceted. *Nat. Rev. Immunol.* **22**, 173–187 (2022).
91. C. Guthrie, G. R. Fink, *Guide to Yeast Genetics and Molecular Biology* (Academic Press, 1991).
92. O. Reuss, A. Vik, R. Kolter, J. Morschhauser, The *SAT1* flipper, an optimized tool for gene disruption in *Candida albicans*. *Gene* **341**, 119–127 (2004).
93. S. M. Noble, A. D. Johnson, Strains and strategies for large-scale gene deletion studies of the diploid human fungal pathogen *Candida albicans*. *Eukaryot. Cell* **4**, 298–309 (2005).
94. M. Gerami-Nejad, L. F. Zacchi, M. McClellan, K. Matter, J. Berman, Shuttle vectors for facile gap repair cloning and integration into a neutral locus in *Candida albicans*. *Microbiology* **159**, 565–579 (2013).
95. S. Dallari, T. Heaney, A. Rosas-Villegas, J. A. Neil, S.-Y. Wong, J. J. Brown, K. Urbanek, C. Herrmann, D. P. Depledge, T. S. Dermody, K. Cadwell, Enteric viruses evoke broad host immune responses resembling those elicited by the bacterial microbiome. *Cell Host Microbe* **29**, 1014–1029.e8 (2021).
96. B. R. Boles, M. Thoendel, A. J. Roth, A. R. Horswill, Identification of genes involved in polysaccharide-independent *Staphylococcus aureus* biofilm formation. *PLOS ONE* **5**, e10146 (2010).
97. M. A. Zafar, M. Kono, Y. Wang, T. Zangari, J. N. Weiser, Infant mouse model for the study of shedding and transmission during streptococcus pneumoniae monoinfection. *Infect. Immun.* **84**, 2714–2722 (2016).
98. W. A. Fonzi, M. Y. Irwin, Isogenic strain construction and gene mapping in *Candida albicans*. *Genetics* **134**, 717–728 (1993).

Acknowledgments: We thank the NYU Grossman School of Medicine Flow Cytometry and Cell Sorting, Microscopy, Genomic Technology, and Histology Cores (supported by NIH grants P31CA016087, S10OD01058, and S10OD018338) and M. Alva, J. Carrasquillo, and D. Basnight of the Gnotobiotics facility for their technical support and use of instruments. **Funding:** This research was supported by NIH grants DK093668 (K.C.), AI121244 (K.C. and V.J.T.), HL123340 (K.C.), AI130945 (K.C.), AI140754 (K.C.), DK124336 (K.C.), and DK122698 (F.Y.), AI140754 (K.C. and V.J.T.), and Intramural Research Program of the NIAID, NIH (P.L.). Additional support was provided by the Faculty Scholar grant from the Howard Hughes Medical Institute (K.C.), Crohn's & Colitis Foundation (K.C. and J.A.), Kenneth Rainin Foundation (K.C.), Judith & Stewart Colton Center of Autoimmunity (K.C. and J.A.), research station and research rebate awards from PU EEB (A.L.G.), National Science Foundation (A.L.G.). K.C. and V.J.T. are a Burroughs Wellcome Fund Investigators in the Pathogenesis of Infectious Diseases. This work was also supported by the Bernard Levine Postdoctoral Research Fellowship in Immunology (Y.-H.C.) and the Charles H. Revson Senior Fellowships in Biomedical Science (Y.-H.C.) and a Cystic Fibrosis Foundation postdoctoral fellowship award LACEY19FO (K.A.L.). **Author contributions:** Design of experiments, data analysis, data discussion, and interpretation: Y.-H.C., F.Y., P.L., A.L.G., and K.C.; primary responsibility for execution of experiments: Y.-H.C., F.Y., K.A.L., K.Z., J.-D.L., and G.C.W.B.; generation of *C. albicans efg1*Δ/Δ and *flo8*Δ/Δ strains: S.-H.L. and R.J.B. Y.-H.C. and K.C. wrote the manuscript with the help of all other authors. **Competing interests:** K.C. has received research support from Pfizer, Takeda, Pacific Biosciences, Genentech, and Abbvie. K.C. has consulted for or received an honoraria from Puretech Health, Genentech, and Abbvie. K.C. is an inventor on U.S. patent 10,722,600 and provisional patent 62/935,035 and 63/157,225. V.J.T. has consulted for Janssen Research & Development LLC, and have received honoraria from Genentech and Medimmune. He is also an inventor on patents and patent applications filed by New York University, which are currently under commercial license to Janssen Biotech Inc. Janssen Biotech Inc. provides research funding and other payments associated with a licensing agreement. **Data and materials availability:** The scRNA sequencing data for this study have been deposited in GEO (GSE231824). Requests for fungal strains should be addressed to K.C. (for wild fungi) or R.J.B. (for *C. albicans*) and should be covered by a material transfer agreement. Requests for *Rorc*$^{-/-}$ mice should be addressed to the donating investigator. All other genetically engineered mice used in this study are commercially available. All data needed to evaluate the conclusions in the paper are present in the paper or the Supplementary Materials.

Submitted 28 June 2022
Accepted 31 May 2023
Published 23 June 2023
10.1126/sciimmunol.add6910